A PILOT STUDY ON THE RHYTHMIC VARIATION IN BLOOD PRESSURE AND PULSE RATE USING STANDARD METHODS OF TIME SERIES ANALYSIS

by

A. Vardy, B.Sc. (London), F.S.S.

Master of Philosophy University of Edinburgh 1975

ABSTRACT

As part of a larger investigation to detect normal patterns in physiological variables records of blood pressure and pulse rate taken from a single patient over a period of fifteen minutes were analysed using standard methods of spectral and cross-spectral analysis. Few indications of normal patterns were found but much was learnt about the problems of examining data of this nature.

Readings extreme in their deviation from their mean but quite natural from a medical viewpoint were found in both series, but there were not sufficient numbers of these observations to investigate in depth a hypothesis that the extremity of deviation of an observation in one series was related to the presence or absence of an observation extreme in the opposite direction at the same point in the second series.

The records were analysed as a whole and as three consecutive blocks of five-minutes in length. Major differences were found in the behaviour of the series between successive blocks, and it was concluded that the variables were not in a sufficient state of equilibrium for the assumption of stationarity to hold.

However there was evidence of the presence of a Mayer cycle in both records, a cycle of length between 20 and 25 seconds, and the two series were highly correlated with blood pressure leading pulse rate by about 11 seconds. Both series also showed evidence of a respiratory cycle of between 3 and 3.5 seconds in length, but the phase shift between the two series was not always the same.

ACKNOWLEDGEMENTS.

The data for this study were supplied by Mr. D.E.M. Taylor of the Department of Physiology, Edinburgh University, whom I would like to thank also for answering any queries I had about the physiological content of the study.

I would like to thank Mr. P.R. Fisk, my supervisor, and Mr. E. Renshaw of the Department of Statistics, Edinburgh University, for advice and helpful discussion throughout.

In the preparation of this dissertation I gratefully acknowledge the help of Dr. P.W. Thomas and Mr. G. Downing of the Computing Laboratory, U.C.N.W. Bangor, in compiling the graphs, and of Mrs. C. McCreadie of Mynydd Llandegai in typing the text.

Finally my thanks go to my wife for her everlasting patience and moral support.

CONTENTS

1. INTRODUCTION

Much of the patient monitoring equipment at present used in intensive care units in hospitals is far from dependable as an automatic warning system for indicating important changes in the condition of the seriously ill patient (Taylor, 1971). The occurrence of false positive alarms is frequent, with the result that a valid alarm can be easily overlooked. One of the main reasons for this shortcoming is a lack of understanding of the characteristics of the signals to be analysed (Taylor et al., 1974 (in press)).

Mr. D.E.M. Taylor and members of the staff of the Department of Physiology, Edinburgh University, have collected substantial amounts of data over the past three years on the pulse rate and arterial blood pressure of a number of patients. These patients were selected at random from patients who had all undergone major open-heart surgery in Edinburgh. This text describes a pilot study on the rhythmic variation in blood pressure and pulse rate, both separately and jointly, using standard methods of spectral and cross-spectral analysis.

The results obtained in this study are based on a record of fifteen minutes in length taken from one patient only. It has been subsequently discovered that the short-term variation of the pulse rate for this patient was much smaller than an average computed from the records of nearly fifty patients, whereas the short-term variation of this patient's blood pressure was much more typical (Taylor and associates, unpublished data). Little weight should be attached to the findings of this investigation as an indication of normal patterns although

some insight is gained into the nature of problems to be expected in examining data of this kind.

Research is to be continued on this material by a post-graduate student within the Department of Physiology, Edinburgh University, as part of a larger project on the nature of normal fluctuations in physiological variables. From this investigation it is hoped to develop methods for the early detection of significant departures from normal patterns in these variables. The patient monitoring sets might then be improved so that complications in a patient's condition would be anticipated and prevented before becoming irreversible.

Past observations on the phasic fluctuations of pulse rate and blood pressure are summarised in Heymans and Neil (1958, pp180-182). Rhythmic variations of blood pressure independent of and slower than the respiration rate were first described by Sigmund Mayer (1876 and 1877), (cited and translated by Heymans and Neil). They are often confused with Traub-Hering waves (sinus arrhythmia) in the literature. Schweitzer (1945) was responsible for clearing up this confusion when he suggested "the following classifications of the main rhythmical fluctuations of the arterial blood pressure.

(1) Fluctuations due to cardiac activity.

(2) Fluctuations due to respiratory activity:

(a) Mechanical effects of the respiratory pump mechanism.

(b) Traub-Hering waves, synchronous with respiration.

(3) Fluctuations which are independent of respiration and always much slower in rate (Mayer waves)."

The Traub-Hering waves (sinus arrhythmia) are observed to have a cycle length of between three and five seconds with respiration, whereas Mayer waves have a cycle length of between twenty and forty seconds. But it must be stressed that these cycles have only been observed in short records and have not been confirmed by any analytical means. There is no evidence that these cycles are exhibited by all humans, and no consideration has been given to their effects if they do occur. In longer records the fluctuations seemingly appear and disappear, and no explanation for this behaviour has been put forward. Hence there exists a real need for a systematic study of the records already available.

.....

2. DESCRIPTION OF DATA

2.1 Collection

The patient from whom the record used in this study was taken had undergone an operation for the replacement of a mitral valve. She was considered to be in a stable clinical state (Taylor et al., 1974 (in press)).

The first step in the preparation of the data was to record continuously onto magnetic tape the electrocardiogram and the arterial blood pressure wave form for a period of eight consecutive hours. Using the coefficient of reliable monitoring suggested by Taylor (1971),

$$\text{viz:-}\quad \frac{\text{time patient reliably monitored}}{\text{total time patient monitored}} \times 100 ,$$

it was found that, over this period of eight hours, the signal was accurate and readable 92.00% of the time for the electrocardiogram and 88.25% of the time for the arterial blood pressure wave form (Taylor and associates, unpublished data).

Each signal was then passed through an identification system, a series of algorithms (where background noise that was deemed not to be signal was identified and removed) and an inspection procedure. If the signal was found to be valid the pulse rate or mean blood pressure was computed on a beat-by-beat basis. If the signal was judged to be unacceptable computation was held at the last valid point before the unacceptable signal, and the signal was flagged.

The paper tape from which the data for this study were taken was then formed by sampling the two variables simultaneously at the rate of one per second, and transforming their values (by multiplying by fifty) to obtain four-digit integers.

All periods containing invalid signals were excluded, except for those described in part (iv) of section 2.3.

2.2 Form of data

The observations on the paper tape are in the form shown in Figure 2.1. The numbers in columns 2-3 and 12-13 represent signal indicators, (00 denotes blood pressure and 02 denotes pulse rate). Columns 5-8 and 15-18 contain the observations for blood pressure and pulse rate respectively, as described in the final paragraph of the previous section. Columns 9 and 19 specify a parity check for each observation, zero being the acceptable value.

2.3 Possible sources of inadmissible data

(i) The signal indicators precede a pair of genuine observations only if columns 2-3 contain 00 and columns 12-13 contain 02. These indicators are used to assess the reliability coefficient (Taylor, 1971) of the signals, and hence periods containing erroneous indicators are omitted from the data tape. (But see (iv)).

(ii) The check for parity fails, i.e. column 9 or column 19 contains an integer other than zero, on average for less than one observation in every ten thousand. This failure is due to a machine fault. No such error was present in the length of record used in this study. (But see (iv)).

(iii) Since the patient concerned was considered to be in a stable clinical state, a blood pressure reading of less than 40 or greater than 120mm.Hg or a pulse rate reading of less than 40 or greater than 150 beats per minute is, in practice, highly implausible. In the terminology of Section 2.2

then, if the blood pressure observation is less than 2000 or greater than 6000, or if the pulse rate observation is less than 2000 or greater than 7500, the pair of observations must be regarded as invalid. These extreme values are thought to be a result of the general problems of using magnetic tape.

(iv) A fault in the inspection equipment, which has since been rectified, permitted some invalid signals to be punched onto the data tape. A typical example of how this error appears on the tape is shown in Figure 2.2. The number of characters printed between the two horizontal lines is around 300 at every occurrence of this fault. Since these characters are punched at the rate of 110 per second it seems reasonable to assume that the lag between the valid observations immediately above line 1 and immediately below line 2 is three seconds.

.....

Figure 2.1. Format of data on the original paper tape.

Column number	1	2,3	4	5-8	9	10,11	12,13	14	15-18	19	20	21 — 80
		00	-	4037	0	.	02	-	2987	0	.	BLANK
		00	-	4177	0	.	02	-	2955	0	.	BLANK
		00	-	3883	0	.	02	-	3003	0	.	BLANK
		00	-	3823	0	.	02	-	2989	0	.	BLANK
		00	-	3735	0	.	02	-	2970	0	.	BLANK

Figure 2.2. A typical example of the result of a fault in the inspection equipment..

00-38410. 02-31230.
00-38370. 02-30830. 1
00-37380. 07-33551. 11-39711. 13-37391. 17-23232.
22-2232. 22-3772. 27-37733. 33-37733. 33-37333.
37-5554. 44-55474. 46-5444. 47-5775. 55-55755.
57-55755. 57-76676. 66-76776. 66-76676. 67-77777.
77-77777. 77-777. 77-998. 88-998. 8-998.
8-999. 99-99. 9-99. 9-13150. 00-34330.
02-26930. 2
00-34050. 02-26930.
00-34400. 02-30090.

3. METHODS

3.1 Computing Techniques

The computer program used in this investigation was the "Autocovariance and Power Spectral Analysis" program, BMD 02T, taken from the Biomedical Computer Programs manual (Dixon, 1967). A general description of the program, the limitations which are applicable in this study, and the computational procedure of the program are given in the Appendix to this dissertation.

As previously noted, Mayer waves are observed to exhibit a cycle length of between twenty and forty seconds. Thus it is desirable to consider a series of at least eight hundred or so observations in order to include enough of these cycles so as to ensure as high a probability as possible that they are accurately detected. Within the limits imposed by the program it seemed reasonable, therefore, to analyse the data in the form of a series of nine hundred observations, or fifteen minutes, in length. However, with a series of this length, it is also desirable to employ a number of lags in excess of 199 (the maximum permitted by the program) to increase the resolution of the spectral estimates (see discussions in Section 3.2.3). Since the number of lags was restricted it appeared reasonable to divide the 900-observation series into three blocks each of 300 observations, and analyse these at the same time as the longer series. In this way it was possible to investigate the properties of the variables in consecutive five-minute intervals, and also to compare these properties with the results obtained by considering a fifteen-minute period.

The first step was to transfer the data from paper tape to punched cards in a form suitable for input to the BMD program as described above. A tape containing the (bivariate) observations 1 - 900 was prepared, and run through a program which replaced all unacceptable values (as defined in Section 2.3) by zero. The resulting observations were punched onto cards, together with their number in the series, in the format shown in Figure 3.1.

The mean of the non-zero pulse rate observations was computed, and all zero pulse rate observations were replaced by this mean. A similar procedure was applied to the blood pressure observations. This produced a series of 900 (bivariate) observations ready for analysis in the BMD program. The original cards (i.e. the set containing the zero observations) were then divided into three blocks, comprising observations 1-300, 301-600 and 601-900, and the above procedure of replacing zeros was repeated for each block in turn. This produced three series each of 300 (bivariate) observations ready for analysis in the BMD program.

These four series of data were then analysed simultaneously using the BMD program, and the results were coded thus:

run A - the analysis of observations 1-300,
run B - " " " " 301-600,
run C - " " " " 601-900,
run D - " " " " 1-900.

Figure 3.1. Format of data for input into the BMD program (on punched cards).

Observation no.	Blood Pressure observation	Pulse Rate observation
98	3613	2940
99	3687	2961
100	3663	2951
101	3807	2958
102	3723	3019

3.2 Theoretical Considerations

3.2.1 Stationarity

The sequence of observations which constitutes the time series to be analysed may be considered as a sampling of an infinite sequence of ordered random variables, known as a stochastic process. Each of these random variables has an associated probability density function. In general the properties of a stochastic process will depend on the time which has elapsed since the start of the process. Matters are much simplified if it is assumed that the series has attained some form of equilibrium, and that the statistical properties of the series are independent of absolute time. A series is said to be weakly stationary or stationary to the second order (henceforward called simply stationary) if the mean and variance of the series are both independent of absolute time and if the covariance between any two points of the series depends only on the time interval between them. Thus a stationary series is one which contains no trends in either its mean or its second order moments.

A series may be said to have an upward trend in the mean if the observations appear to fluctuate about a continually increasing value. A trend in variance is present if the extent of the fluctuation of observations about the mean changes with time. A third and more complicated type of trend, which is rarely visible, is a change in the correlation between successive values with time.

3.2.2 Autocovariance

As noted above the assumption of stationarity means that the general formula for autocovariance,

$$\mathcal{R}_x^{(t_1,t_2)} = E[(X'_{t_1} - \mu_{t_1})(X'_{t_2} - \mu_{t_2})],$$

can be simplified to $\mathcal{R}_x^{(p)} = E[(X'_t - \mu)(X'_{t+p} - \mu)]$ to depend only on p, the lag or interval $t_2 - t_1$. (A full glossary of the symbols used in this dissertation is given in the Appendix.) The autocovariance at lag p is computed in the program by the formula

$$R_x^{(p)} = \frac{1}{n-p}\sum_{q=1}^{n-p} X_q X_{q+p} \quad , \quad p = 0, 1, \ldots\ldots, m,$$

where X_i is the i^{th} value of the series after subtraction of the mean and m is the number of lags chosen, (discussed in Section 3.2.3).

Another formula in common use is

$$R_x'^{(p)} = \frac{1}{n}\sum_{q=1}^{n-p} X_q X_{q+p} \quad , \quad p = 0, 1, \ldots\ldots, m.$$

When considered as estimators of the theoretical autocovariance, $\mathcal{R}_x^{(p)}$, of the stochastic process, both are primarily based on intuitive appeal. The advantage of $R_x^{(p)}$ is that it is unbiased but Jenkins and Watts (1968, pp171-189) have found that $R_x'^{(p)}$ has a smaller mean square error.

The plot of $R_x^{(p)}$ against p is called the autocovariance function of the time series, and shows how the dependence of adjacent values alters with lag p. For the comparison of series of different scales of measurement it is wise to normalize the autocovariance function by dividing it by $R_x^{(o)}$, the variance of the time series. The autocorrelation function is defined by

$$r_x^{(p)} = R_x^{(p)} / R_x^{(0)}.$$

It can easily be shown that

$$-1 \leq r_x^{(p)} \leq 1 \quad \text{for all } p.$$

3.2.3 Estimation of the power spectrum

In theory a series containing a deterministic harmonic term has an autocovariance function which is also harmonic and does not damp out, as opposed to random data which has an autocovariance function which diminishes to zero as the lag increases, and thus the autocovariance function should provide a tool for detecting periodicity in a time series. But in practice this is not generally the case. Correlation between neighbouring values of the series may distort the shape of the function near the origin and also mask its behaviour at longer lags so that any periodicities in the series cannot be detected with sufficient accuracy. One of the main objectives of this study was to investigate cycles in the input data. The autocovariance functions computed in the analyses provide no conclusive information about these periodicities (see Section 4.3). Some other measure is needed to attempt to give a clearer picture of the behaviour of the input data.

The Fourier transform of the autocovariance function is called the power spectrum. It follows from the relationship between these two functions that each contains the same information about the time series as the other. The power spectrum shows how the variance of the series is distributed over the frequency of possible harmonic components. In other words, it isolates the contribution to the variance of each frequency

band.

In the analysis of series of finite length the spectrum is preferable to the autocovariance function for interpretation purposes. The choice of m, the maximum number of lags, can be made such that the power spectral estimates at neighbouring frequencies are approximately independent, and as a result it is usually easier to detect periodic components from the estimate of the power spectrum than from the autocovariance function. The frequencies of these components can also be more accurately estimated.

The basic relationship between the power spectral estimator and the sample autocovariance function is the same as that between their theoretical counterparts, namely the Fourier transform. However, slight modifications are necessary to improve the ability of the estimator to reflect accurately the true power spectrum.

The raw estimate of the power spectrum is given in the BMD program by the formula

$$P_x^{(h)} = \frac{2\Delta t}{\pi} \sum_{p=0}^{m} \varepsilon_p R_x^{(p)} \cos \frac{hp\pi}{m} \quad , \quad h = 0, 1, \ldots, m \quad ,$$

where

Δt = the constant time interval between consecutive points in the series,

$$\varepsilon_p = \begin{cases} 1 & 0 \; p \; m \\ \frac{1}{2} & p=0,m \end{cases}$$

and m = the maximum number of lags chosen.

It can be shown that if the series is stationary $R_x^{(p)} = R_x^{(-p)}$, i.e. that, in theory, autocovariance is an even

function of lag. Since the cosine function is also even, if $R_x^{(p)}$ is defined to equal $R_x^{(-p)}$,

$$P_x^{(h)} = \frac{\Delta t}{\pi} \sum_{p=-m}^{m} \omega_p R_x^{(p)} \cos \frac{hp\pi}{m} \quad , \quad h = 0, 1, \ldots\ldots, m \quad ,$$

where

$$\omega_p = \begin{cases} 1 & |p| < m \\ \frac{1}{2} & p = -m, m \\ 0 & |p| > m \end{cases} .$$

In this study $\Delta t = 1$, so

$$P_x^{(h)} = \frac{1}{\pi} \sum_{p=-m}^{m} \omega_p R_x^{(p)} \cos \frac{hp\pi}{m} \quad , \quad h = 0, 1, \ldots\ldots, m \quad .$$

The function ω_p is called a data window. A full discussion of this concept and its uses is given in Jenkins and Watts (1968, pp48-50) and Anderson (1958, pp508-18). The considerations here are related purely to the data window used in this study.

The window ω_p has a fixed rectangular shape with width 2m. The program allows m to be chosen, with a maximum value of 199. Both the width and shape of the window affect the form of the power spectral estimator. The rectangular shape of the window can cause several false peaks between the main real peaks, and this is unavoidable. However, peaks of the power spectrum at frequencies near to each other are separated by a rectangular window half as wide as that which would be necessary for a non-rectangular window to be able to perform the same task. A rectangular window of width 2m can separate peaks at frequencies differing by $1/m$ c.p.s. Regardless of the shape of the window, separate peaks of the power spectrum at frequencies

near together are fused into a single peak if the data window is too narrow. For example, if the true power spectrum contained two distinct peaks separated by less than $1/m$ c.p.s. then the power spectral estimator using a rectangular window of width 2m would not be able to distinguish between the two peaks, and would produce a single peak only in the range of frequency concerned. The width of the window also affects the bias and the variance of the power spectral estimator. If m is small then so is the variance of the power spectral estimator, but its bias may be large. If m is made large to reduce the bias then the variance is increased. Some form of compromise therefore must be reached. Jenkins and Watts (pp240-8) discuss this problem in greater detail in their book.

In runs A, B and C, which analysed series of 300 observations each, the chosen value of m was 100. This choice ensured that the estimator could detect peaks of the power spectrum very close to each other, and also that the estimator had small bias. But the choice reduced the variance of a completely raw estimator (the Fourier transform of the autocovariance function without the data window) by approximately one third only (Jenkins and Watts, p252). In order to see the effect of narrowing the data window, and thus reducing the variance but increasing the bias of the power spectral estimator, the analysis of observations 1-300 was repeated using a maximum lag of 60 seconds (run G) and the results compared with those of run A. In run D, which analysed the 900 observation series, the chosen value of m was 199, the maximum allowed by the program. In comparison with runs A, B and C, assuming

the series to be homogeneous and stationary (see Sections 4.2 and 5.2), the variance is further reduced (to about 45% of that of a completely raw estimator), and since the length of record has been trebled and the data window width only doubled it is likely that the bias of the estimator has also been reduced.

A further process designed to reduce the variance of the power spectral estimator is that of smoothing. The raw power spectral estimate at a certain frequency is replaced by a weighted average of estimates at and near that frequency. In this way it is hoped that variation caused mainly by the fact that a finite series is being used can be reduced. Thus the irregular graph of raw power spectral estimates is replaced by a smoother graph. The procedure used in the BMD program is "hamming", which smooths the power spectral estimates according to the formulae

$$SP_x^{(0)} = 0\cdot54P_x^{(0)} + 0\cdot46P_x^{(1)},$$

$$SP_x^{(h)} = 0\cdot23P_x^{(h-1)} + 0\cdot54P_x^{(h)} + 0\cdot23P_x^{(h+1)}, \quad 0<h<m,$$

$$SP_x^{(m)} = 0\cdot54P_x^{(m)} + 0\cdot46P_x^{(m-1)}.$$

Jenkins and Watts (pp243-257) and Anderson (pp508-18) both give a detailed discussion of "hamming" and other smoothing procedures.

The stage has now been reached where the power spectral estimates have been computed and smoothed, and it is hoped that the resulting graphs are a reasonable representation of the corresponding theoretical power spectrum. Before interpretations are made, since series are being compared which are likely to have unequal variances, it is useful to normalize the

power spectral estimates of each series by dividing them by the variance of that series. The resulting function is the estimator of the spectral density function.

3.2.4 Cross-covariance

The cross-covariance is computed by the formulae

$$R_{xy}^{(p)} = \frac{1}{n-p} \sum_{q=1}^{n-p} X_q Y_{q+p} \quad , \quad p = 0, 1, \ldots\ldots, m \quad ,$$

$$R_{xy}^{(-p)} = \frac{1}{n-p} \sum_{q=1}^{n-p} X_{q+p} Y_q \quad , \quad p = 0, 1, \ldots\ldots, m \quad .$$

In common use also, as in the univariate case of autocovariance, are the formulae which use n (instead of n-p) as the divisor. The advantages and disadvantages connected with the different divisors have been mentioned in Section 3.2.2 in relation to autocovariance, and the same considerations apply to cross-covariance.

The plot of $R_{xy}^{(p)}$ against p is called the cross-covariance function. It measures the degree of correlation between the X_t series (blood pressure), lagged p seconds, and the Y_t series (pulse rate). In theory $R_{xy}^{(p)} = R_{yx}^{(-p)}$, and if this equality is defined to hold for the sample statistics the description of cross-covariance holds with the series interchanged when $R_{yx}^{(p)}$ is plotted against p. In practice it is necessary to study the interactions between two processes with different variances. In this situation the cross-covariance function must be normalized by defining the cross-correlation function

$$r_{xy}^{(p)} = R_{xy}^{(p)} \; / \; R_x^{(o)} \cdot R_y^{(o)} \quad , \quad p = -m, \ldots\ldots, -1, 0, 1, \ldots\ldots, m$$

where

$$\left| r_{xy}^{(p)} \right| \leq 1 \ .$$

3.2.5 Estimation of the Cross-Spectrum and Coherence Squared

As was found in the case of the univariate autocovariance function, it is very difficult to interpret the cross-covariance function. If adjacent points of the two time series are cross-correlated it is found that the cross-covariance function is large near the origin (p=0) and small at values distant from the origin. But if the cross-covariance function contains periodic components these may not easily be detected from the graph. It follows that some other measure is needed to clarify the relationship between the series.

The Fourier transform of the cross-covariance function is called the cross-spectrum. Because the cross-covariance is not an even function, the cross-spectrum is generally a complex quantity which may be written as a sum of a real part, the cospectrum, and an imaginary part, the quadrature spectrum. The cospectrum is an even function of frequency and can be thought of as the average product of X_t and Y_t within a narrow frequency interval, divided by the frequency interval. In other words the cospectrum measures the covariance between the in-phase components of the series. The quadrature spectrum is an odd function of frequency and can be thought of in the same terms as the cospectrum except that either X_t or Y_t, not both, is shifted in time sufficiently to produce a 90-degree phase shift at frequency f. In other words the quadrature spectrum measures the covariance between out of phase components. (For

proofs and further discussions of these results see Jenkins and Watts, pp343-4).

In estimating the cross-spectrum from two series of finite length, the same problems of variance and bias which were discussed in Section 3.2.3 arise. Hence the cross-spectral estimator must be computed using a data window and a smoothing procedure. The considerations given to the data window and smoothing procedure in Section 3.2.3 apply here, but there is one important difference. The autocovariance function is an even function of lag, being symmetric about p=0, and if it damps out quickly it should be possible to reduce substantially the bias of the power spectral estimator by increasing the width of the data window. But the cross-covariance is not an even function of lag and is therefore not symmetrical about p=0. Thus in the case of one series leading the other exactly by an amount τ the data window must be wide enough to account for this delay, or very appreciable bias will result. In this study the windows used in the estimation of the cross-spectrum are those described in Section 3.2.3.

The estimates of the cospectrum in this study are obtained from

$$C_{xy}^{(h)} = \frac{1}{\pi} \sum_{p=0}^{m} \varepsilon_p \left(R_{xy}^{(p)} + R_{xy}^{(-p)} \right) \cos \frac{hp\pi}{m} \quad , \quad h = 0, 1, \ldots\ldots, m \quad ,$$

where

$$\varepsilon_p = \begin{cases} 1 & 0<p<m \\ \frac{1}{2} & p=0, m \end{cases} \quad ,$$

and then smoothed by "hamming". The results are printed but not plotted by the BMD program. The estimates of the quadrature spectrum are obtained from

$$Q_{xy}^{(h)} = \frac{1}{\pi}\sum_{p=0}^{m} \varepsilon_p \left(R_{xy}^{(p)} - R_{xy}^{(-p)}\right) \sin\frac{hp\pi}{m} \quad , \quad h = 0, 1, \ldots\ldots, m \quad ,$$

where

$$\varepsilon_p = \begin{cases} 1 & 0<p<m \\ \frac{1}{2} & p=0, m \end{cases} \quad ,$$

and also smoothed by "hamming". Again the results are printed but not plotted. The cross-spectrum, $SP_{xy}^{(h)}$, is given by

$$SP_{xy}^{(h)} = SC_{xy}^{(h)} + iSQ_{xy}^{(h)}$$

where S denotes smoothing.

An alternative way of expressing the cross-spectrum is in a complex polar form, by the product of a real function, $AM_{xy}^{(h)}$, called the cross amplitude spectrum, and a complex function, $e^{iPHAS_{xy}^{(h)}}$, where $PHAS_{xy}^{(h)}$, is called the phase spectrum. The cross amplitude spectrum shows whether frequency components in one series are associated with large or small amplitudes at the same frequency in the other series. Similarly, the phase spectrum describes the manner in which frequency components in one series lag or lead the components at the same frequency in the other series.

In this study, having computed the cross-spectral estimates, the amplitude of the cross-spectrum is given by

$$AM_{xy}^{(h)} = \sqrt{(SC_{xy}^{(h)})^2 + (SQ_{xy}^{(h)})^2}$$

and the phase of the cross-spectrum by

$$PHAS_{xy}^{(h)} = Arg\,(SP_{xy}^{(h)}) .$$

The phase angle computed at each frequency is the phase shift of the pulse rate series with respect to the blood pressure series (See Appendix).

To investigate the correlation between two time series at each frequency a measure called the coherence squared is used in preference to the amplitude of the cross-spectrum. The coherence squared at each frequency is computed by squaring the amplitude of the cross-spectrum at that frequency and dividing by the product of the power-spectrum of each series at that frequency. The coherence squared resembles a correlation coefficient at each frequency in that it is a measure of the linear relation between the spectral variates of the two series at that frequency. In a comparison such as the one in this study the coherence squared is preferred to the amplitude of the cross-spectrum because it is an absolute measure whereas the amplitude of the cross-spectrum depends on the variances of the two time series concerned (cf covariance and correlation coefficient).

The coherence squared gives information about the linear association between the two series at each frequency, and the phase spectrum shows by how much one series lags or leads the other at each frequency. Thus these two measures adequately describe any linear relationships between the two series.

3.3 Further experiments

On looking at the graph of observations 1-900 (Figures

4.1(a) and 4.1(b)) it can be seen that the final 20 observations fluctuate much more wildly than the remainder both for blood pressure and pulse rate. In order to discover if these extreme values had a large effect on the analysis of the fifteen-minute series of observations (run D) the series consisting of observations 1-880 was also analysed (run E). This involved a recomputation of the means for both variables and a substitution of these new means for unacceptable values within the 880 observation series.

The graphs of the power spectral estimates resulting from the analysis of this series showed a marked peak at the origin for both the pulse rate and blood pressure series, indicating the possibility of a trend in the input data. The analysis of the 880 observation series was thus repeated after detrending the input series (run F) in the way described in the Appendix.

Finally the first block of 300 observations was reanalysed (run G) using 60 lags instead of 100 as a comparison with run A. This was done in order to see the effect of reducing the number of lags, thus reducing the resolution of the power spectral estimates but increasing their stability.

A summary of all the analyses performed on the data using the BMD program is given in Table 3.1.

.....

Table 3.1. A summary of the analyses performed on the data set using the BMD program.

Job Code	Observations analysed	Was data printed and plotted?	Was detrending performed?	Was pre-whitening used?	Chosen no. of lags
A	1-300	Yes	No	No	100
B	301-600	Yes	No	No	100
C	601-900	Yes	No	No	100
D	1-900	Yes	No	No	199
E	1-880	Yes	No	No	199
F	1-880	No	Yes	No	199
G	1-300	No	No	No	60

4. RESULTS

4.1 Extreme Values

It was immediately apparent on inspection of the input data for the whole fifteen-minute period (Figures 4.1(a) and 4.1(b)) that the series of both variables contained observations which, although perfectly acceptable, were nevertheless extreme. In the case of pulse rate this phenomenon occurs when the heart gives out an extra abnormal beat, producing a short interval between consecutive heartbeats and thus a high pulse rate reading. On occasion this short interval is followed by a correspondingly long interval, which gives a low reading immediately following the high one. Alternatively, the interval length may return instantly to normal, and the only record of the extra beat remains the single high pulse rate observation. Sometimes the short interval is not sampled in the procedure described earlier (p.4) but the following long interval is, resulting in one low pulse rate reading.

The extra beat may or may not affect the blood pressure wave form. If it does the result is a blood pressure value at the corresponding point in the pulse rate series which is extreme in the opposite direction. Extreme values of blood pressure are also caused by other factors such as sharp breathing and may not be reflected in the pulse rate series.

The important point to be made here is that this phenomenon is regarded as normal by the medical profession.

A summary of extreme values found in the data of this study is given here together with an attempt to discover whether there is any evidence to support a theory that the extent of

extremity of an observation is related to the probability that the observation is balanced by a value of the opposite extreme. These results relate to the series of 900 observations. Inclusion of the final 20 observations is open to question.

To the nearest integer,

Blood pressure	mean	=	3751 (= 75.02mm.Hg)
	standard deviation	=	262 (= 5.24mm.Hg)
Pulse rate	mean	=	2998 (=59.96 beats per minute)
	standard deviation	=	288 (= 5.76 beats per minute).

Any value greater than two standard deviations from the mean (roughly denoting the 95% probability limits of the Normal distribution*) was noted. These observations were then divided into those between two and three standard deviations from the mean and those greater than three standard deviations from the mean (the latter point roughly denoting the 99.9% probability limits of the Normal distribution*). Since both records were made simultaneously, so that identical observation numbers correspond to identical times, it was then easy to discover whether or not each of these observations was balanced by an observation of the opposite extreme, either immediately following in the same series or at the same point in the series denoting the other variable under consideration.

* At the time of this study no investigation has been made into the distribution of the blood pressure and pulse rate measurements. The intervals noted here were chosen simply because they were the intervals used by the staff of the Department of Physiology in their work in this area (Section 5.1).

A list of these extreme observations, tabulated according to whether or not each observation was balanced, is given in Tables 4.1(a) and 4.2.

A 2x2 table, constructed from the data of Table 4.1(a), with classification by number of standard deviations from the mean, is presented as Table 4.1(b). The only striking feature of this table is the large proportion of balanced observations and corresponding balancing observations greater than three standard deviations from the mean.

Two further tables (4.3(a) and 4.3(b)) were produced by classifying for each variable the extremity of deviation against the presence or absence of a balancing observation. All that was learnt from the pulse rate table was that a very high proportion of the extreme observations were greater than three standard deviations from the mean. But the blood pressure results did contain some evidence to suggest that an unbalanced observation was more likely to be between two and three standard deviations from the mean than a balanced observation.

Table 4.1(a). Extreme observations balanced by an observation extreme in the opposite direction.

Pulse Rate		Blood Pressure	
Observation number	No. of s.d.'s from mean	Observation number	No. of s.d's from mean
145	3+	145	3+
210	3+	211	3+
373	3+	373	3+
437	2-3	437	3+
468	2-3	468	2-3
623	3+	623	2-3
697	3+	697	3+
703	3+	703	3+
892	3+	892	2-3
893	3+	893	2-3
894	3+	894	3+
898	3+	898	3+

Table 4.1(b). Balanced extreme observations classified by extremity of deviation from the mean.

		BLOOD PRESSURE		TOTALS
	No. of s.d.'s from mean	2-3	3+	
PULSE RATE	2-3	1	1	2
	3+	3	7	10
TOTALS		4	8	12

Table 4.2 Unbalanced extreme observations.

Pulse Rate		Blood Pressure	
Observation no.	No. of s.d.'s from mean	Observation no.	No. of s.d.'s from mean
74	3+	265	2-3
138	3+	273	2-3
146	3+	315	2-3
164	3+	335	3+
166	3+	381	2-3
370	3+	394	2-3
445	3+	406	2-3
505	3+	413	3+
600	3+	414	3+
810	3+	449	3+
883	3+	526	3+
884	3+	561	3+
886	3+	564	2-3
887	3+	566	2-3
888	3+	571	3+
889	3+	575	2-3
		592	3+
		665	2-3
		680	3+
		741	2-3
		742	2-3
		747	3+
		748	2-3

Table 4.3 Extreme observations classified by extremity of deviation from the mean and by presence or absence of a balancing observation.

(a) Pulse Rate.

		Balancing Observation		Totals
		Present	Absent	
No. of s.d.'s from mean	2-3	2	0	2
	3+	10	16	26
Totals		12	16	28

(b) Blood Pressure.

		Balancing Observation		Totals
		Present	Absent	
No. of s.d.'s from mean	2-3	4	13	17
	3+	8	10	18
Totals		12	23	35

4.2 Stationarity

A cursory examination of the input data for this study, shown in Figures 4.1(a) and 4.1(b), showed no obvious signs of non-stationarity. The mean value of each variable appeared to remain sufficiently constant with time, and the observations did not appear to change their extent of variability about their mean. Therefore it appeared reasonable to analyse these data on the assumption that both series were stationary.

4.3 Autocovariance and Power Spectral Analysis

An examination of the autocovariance functions produced in the various analyses of the data showed, in general, very little correlation between neighbouring observations. The highest value of the autocorrelation function was 0.43 at a lag of one second for the pulse rate observations 601-900, and in every case the autocorrelation function hardly deviated from zero after a lag of about 20 seconds.

Figures 4.2(a) and 4.2(b) show the graphs of the power spectral estimates, plotted against frequency, of blood pressure and pulse rate respectively, computed from observations 1-300 with m=100. In the case of blood pressure there is one marked peak at a frequency of 0.275 c.p.s., a cycle of length 3.6 seconds, which almost certainly represents a respiratory cycle. The spectral density at this frequency is 1.63. The next highest peak occurs at a frequency of 0.110 c.p.s., a cycle of length 9.1 seconds, with spectral density 0.81. In the range of the Mayer cycle, 0.025 c.p.s. to 0.050 c.p.s., the maximum value of the spectral density is 0.64, at a frequency of 0.030 c.p.s. In contrast, the graph of the power spectral

FIGURE 4.1(a). Transformed Blood Pressure readings plotted against their number in the series.

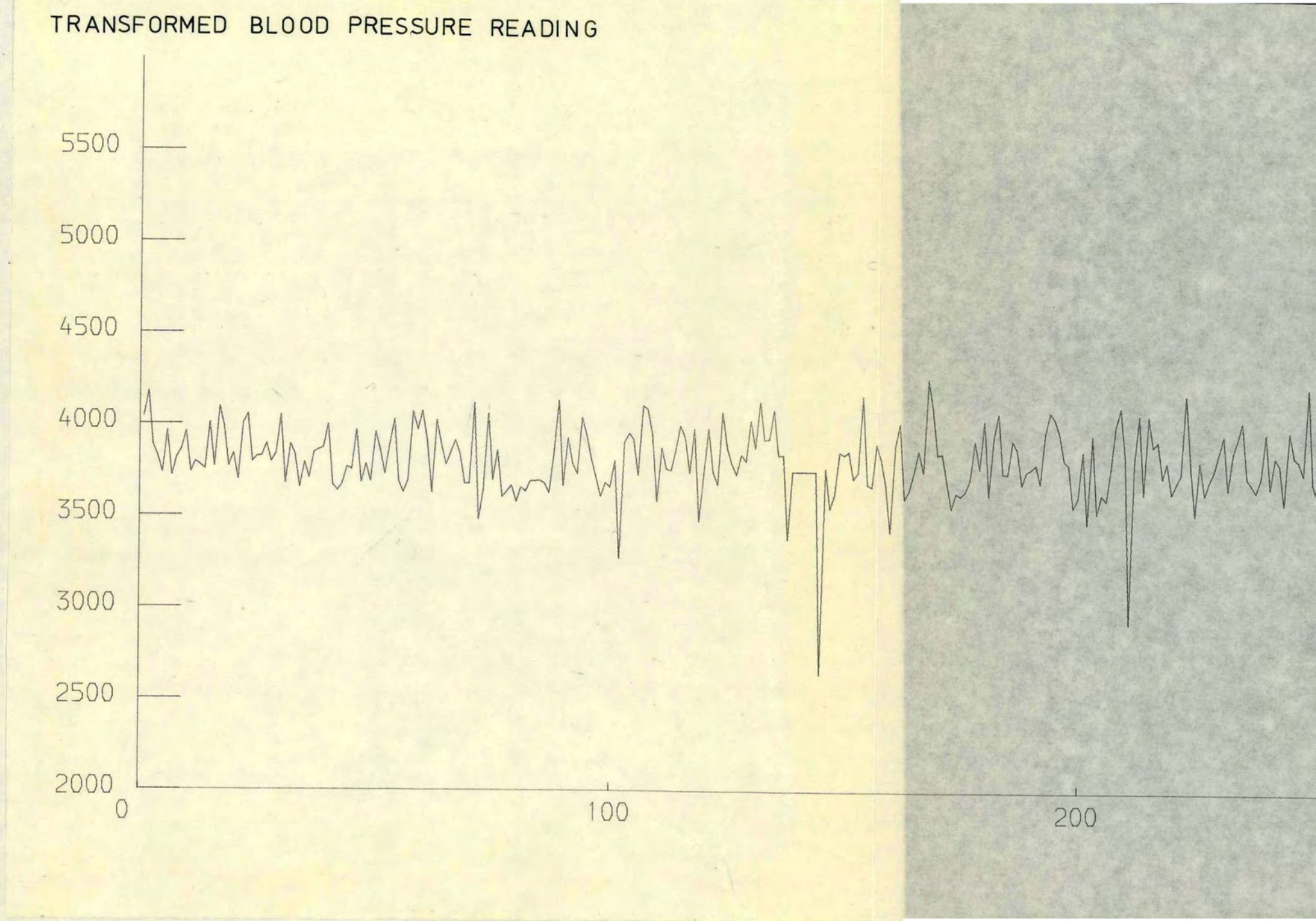

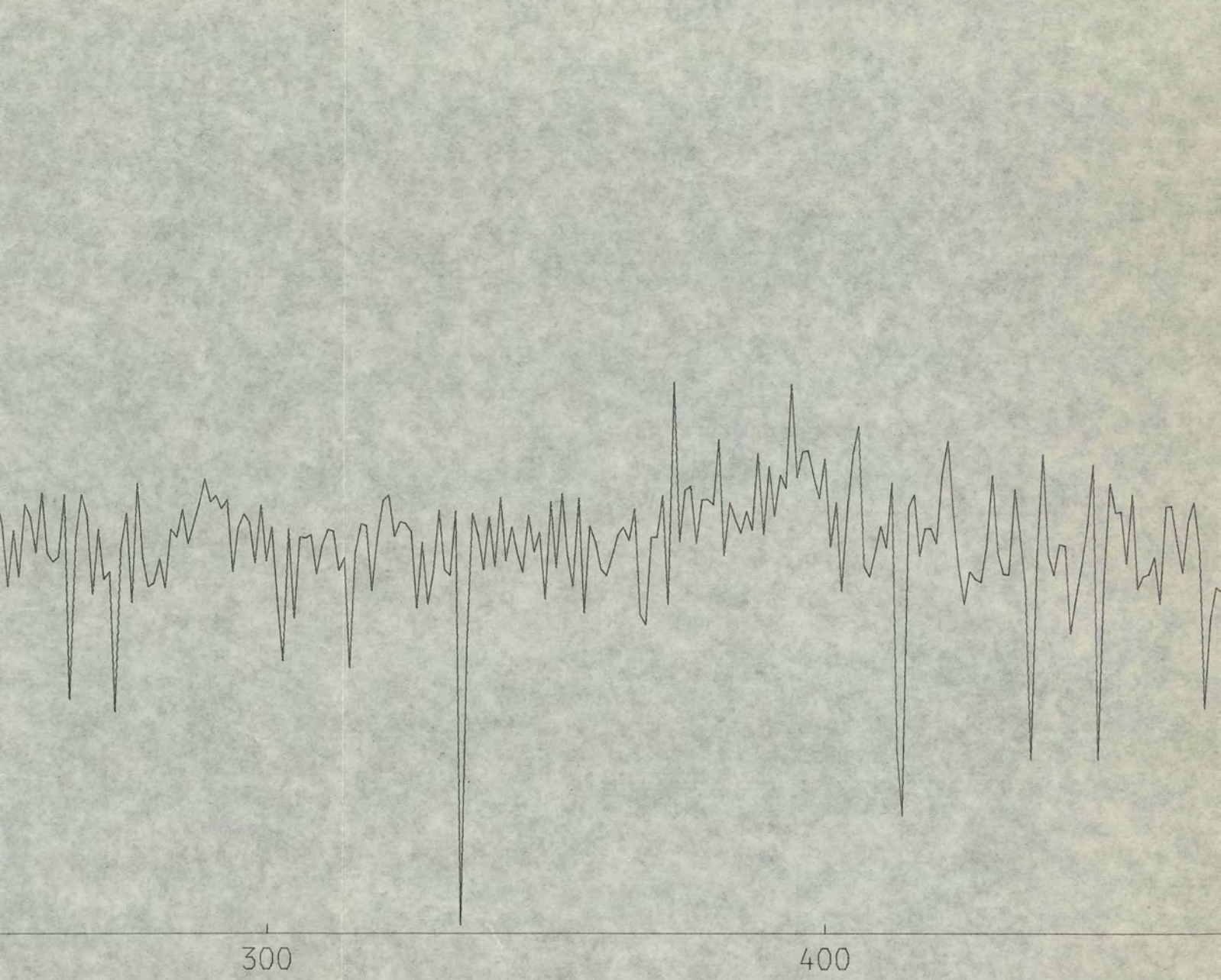
300
400
NUMBER IN SERIES

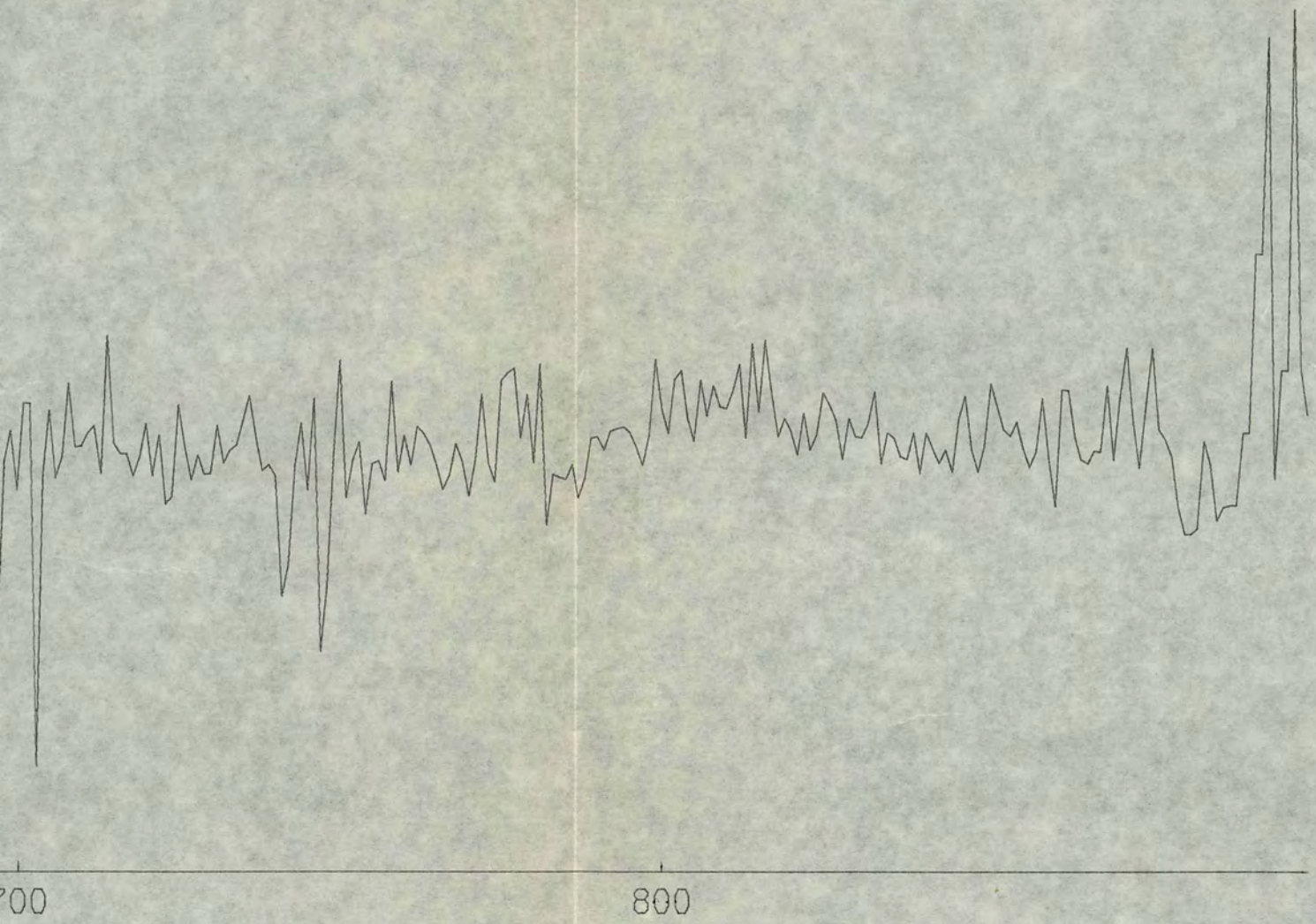
700
800

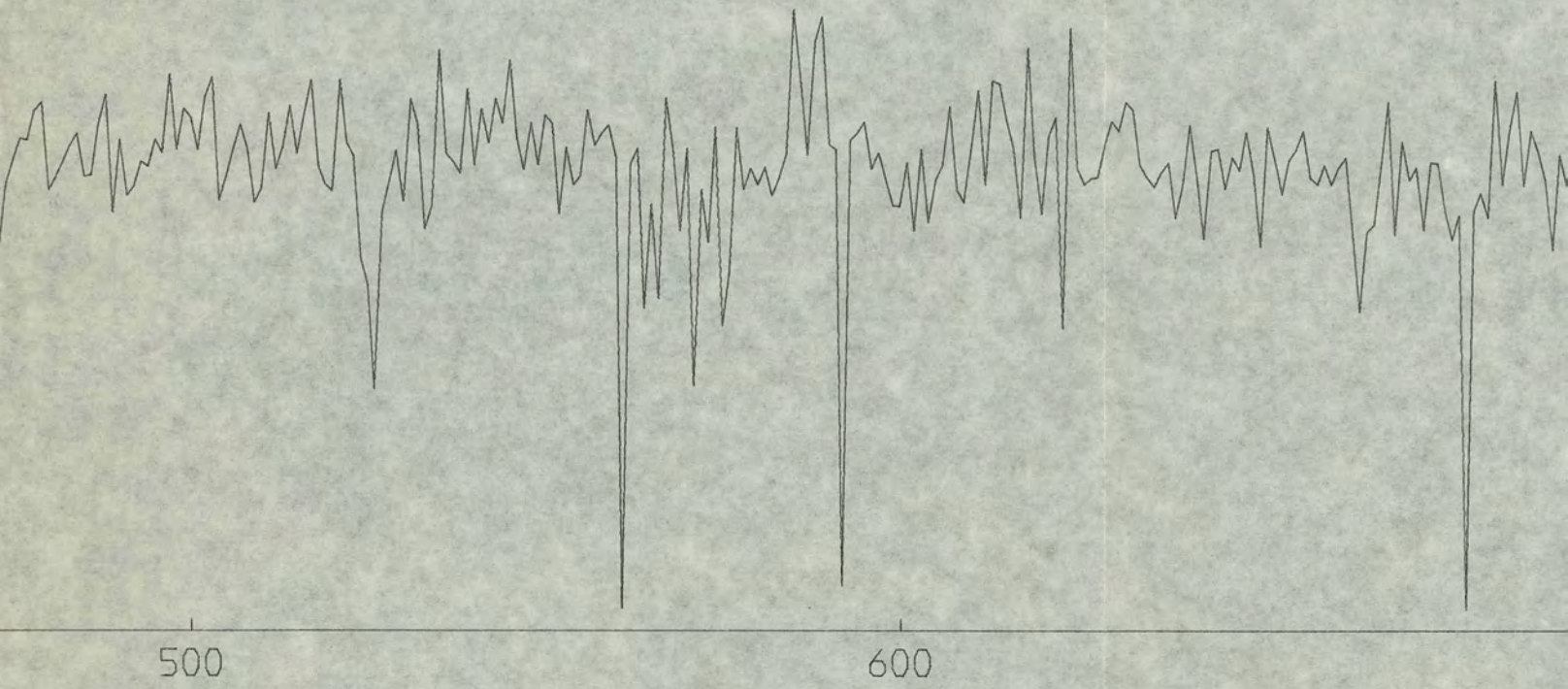
500
600

FIGURE 4.1(b). Transformed Pulse Rate readings plotted against their number in the series.

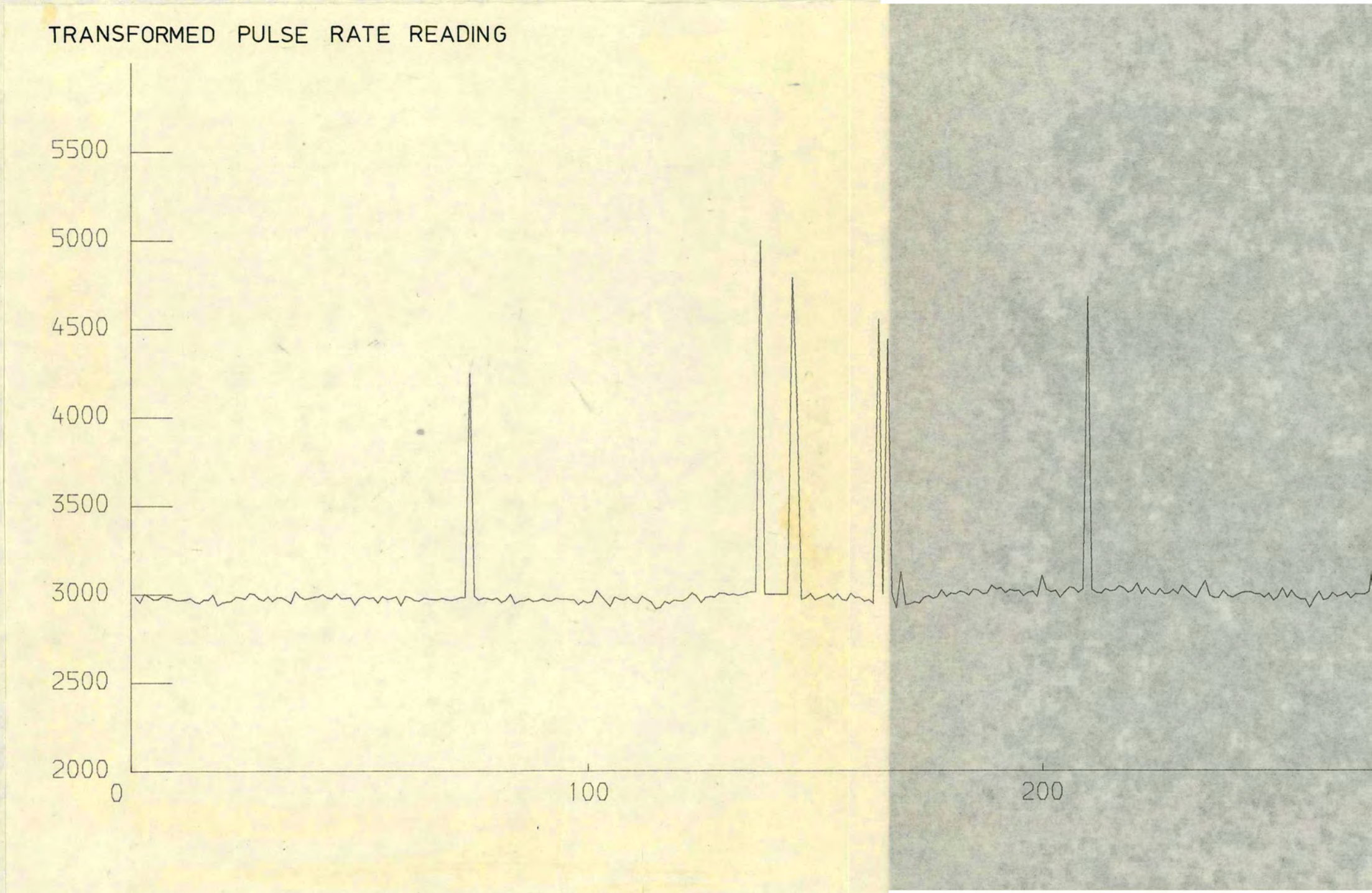

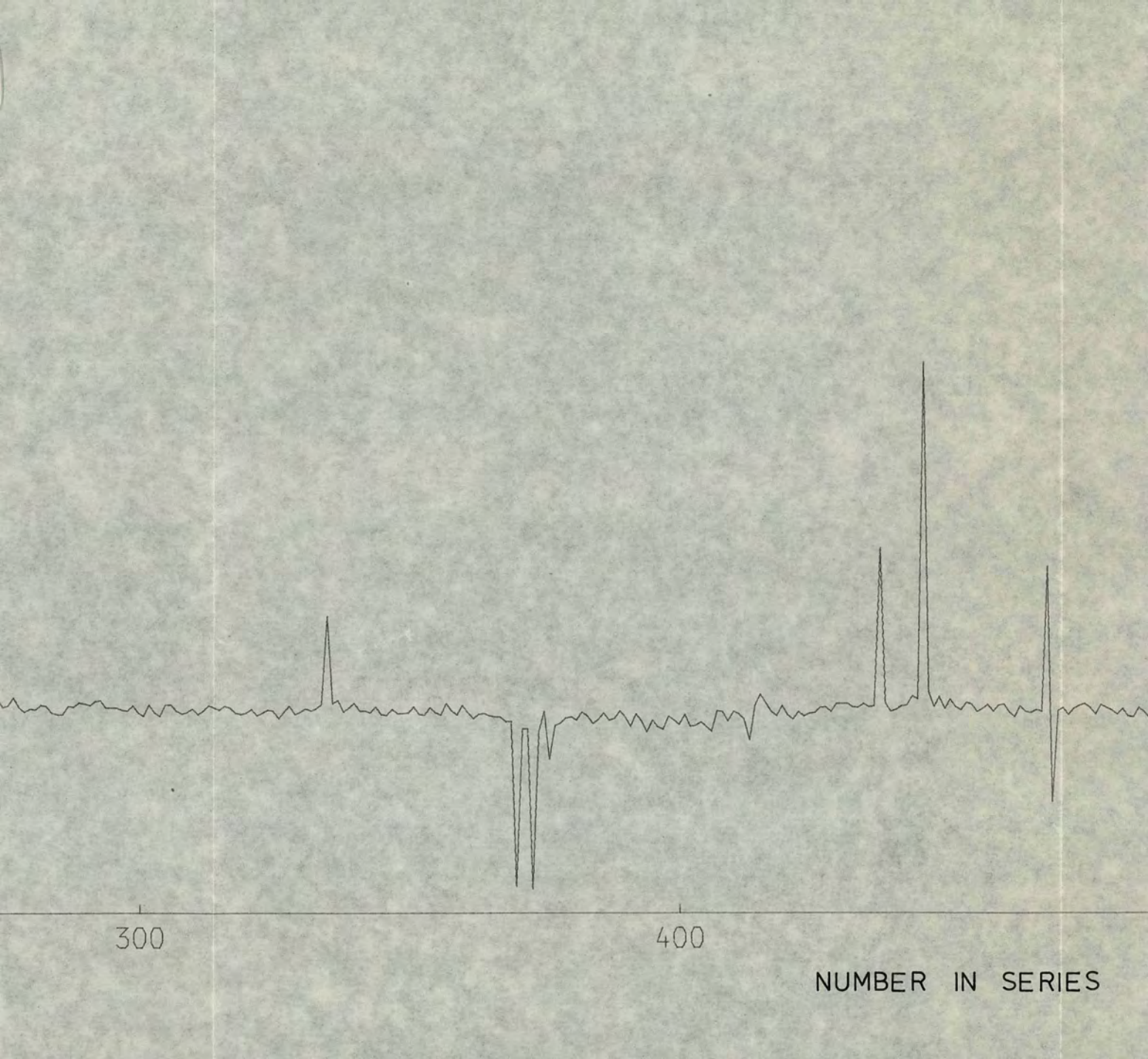
300
400
NUMBER IN SERIES

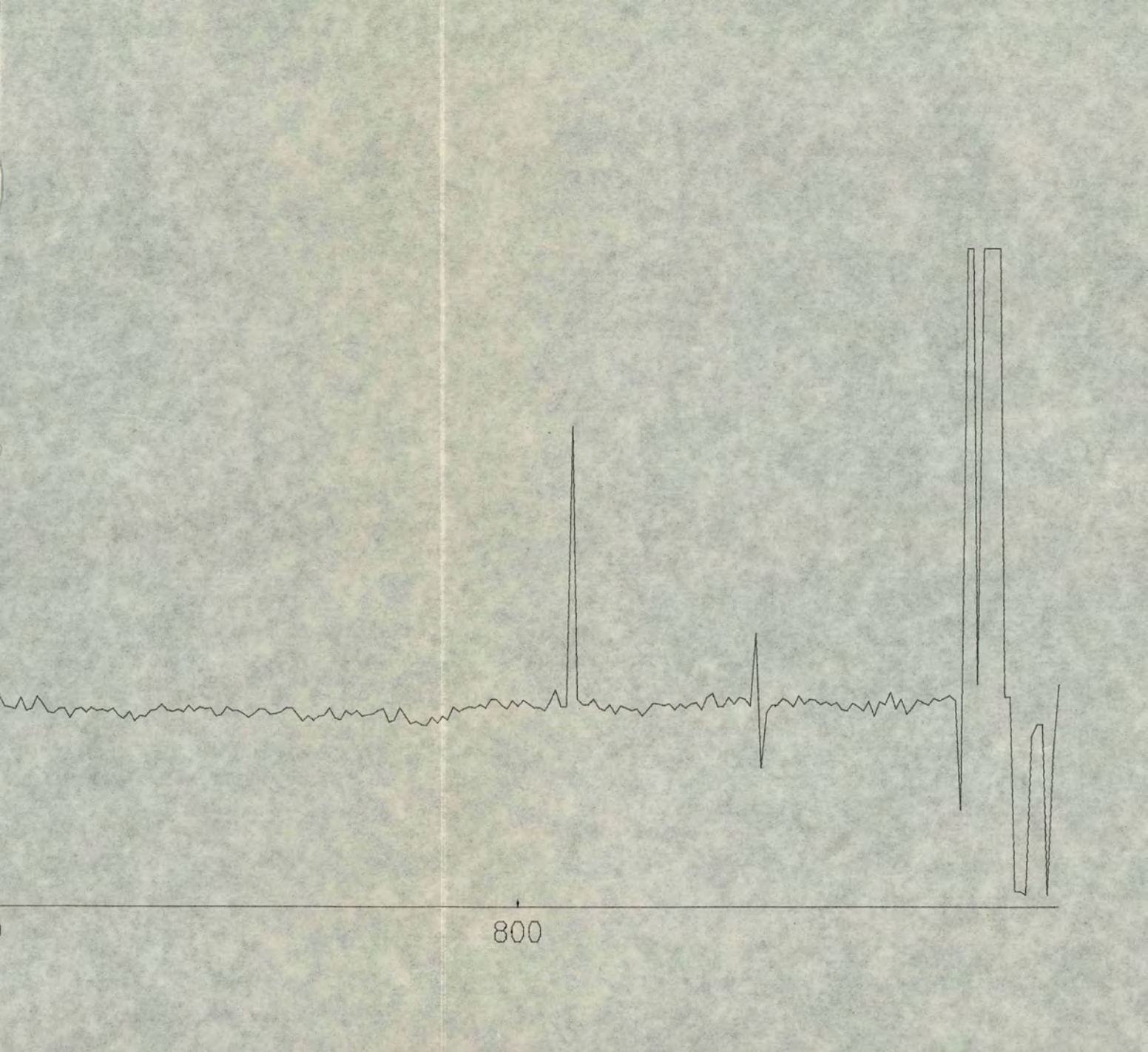
800

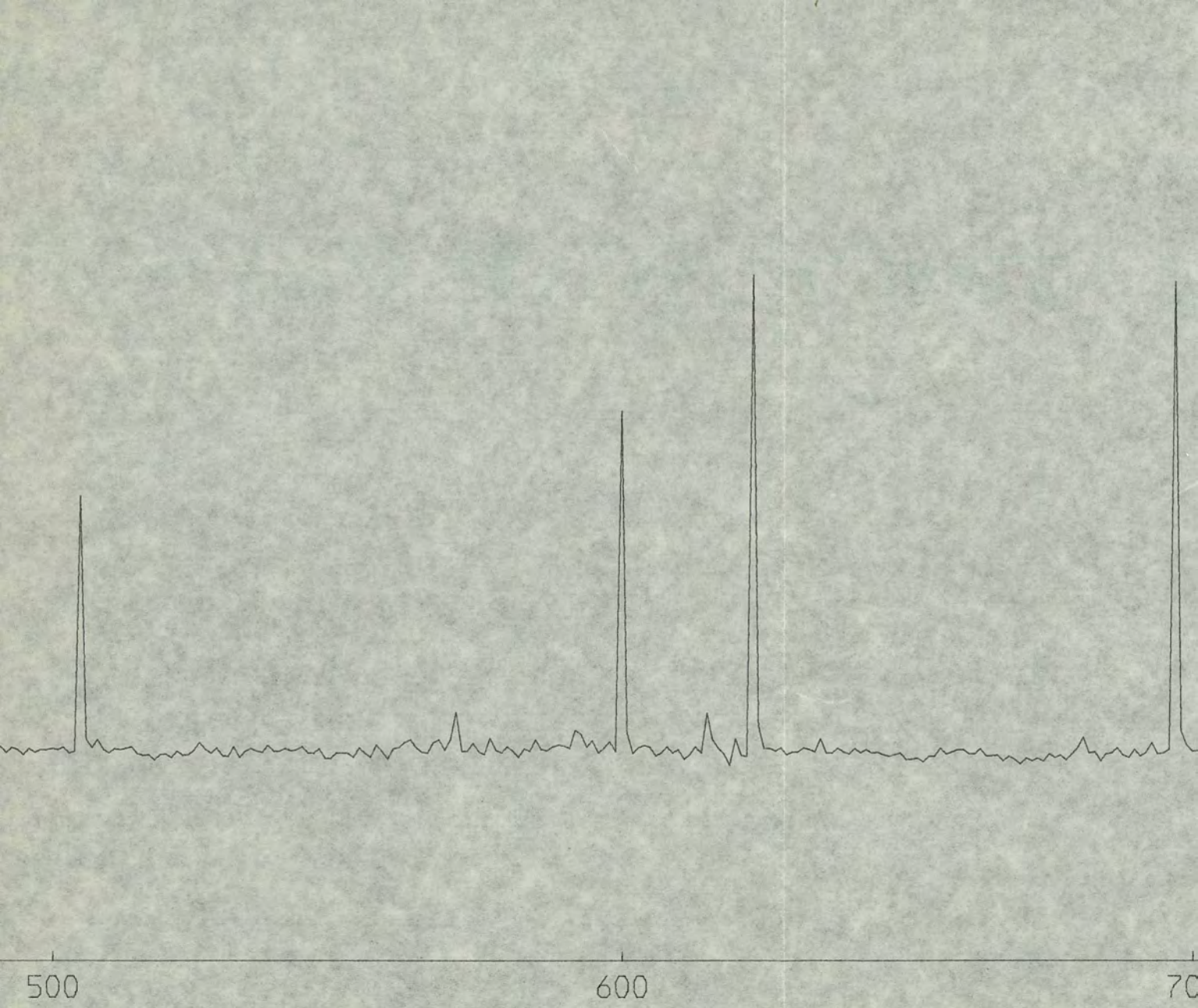
500
600
70

FIGURE 4.2(a). Power spectral estimates of blood pressure series computed from observations 1-300 (m=100) plotted against frequency.

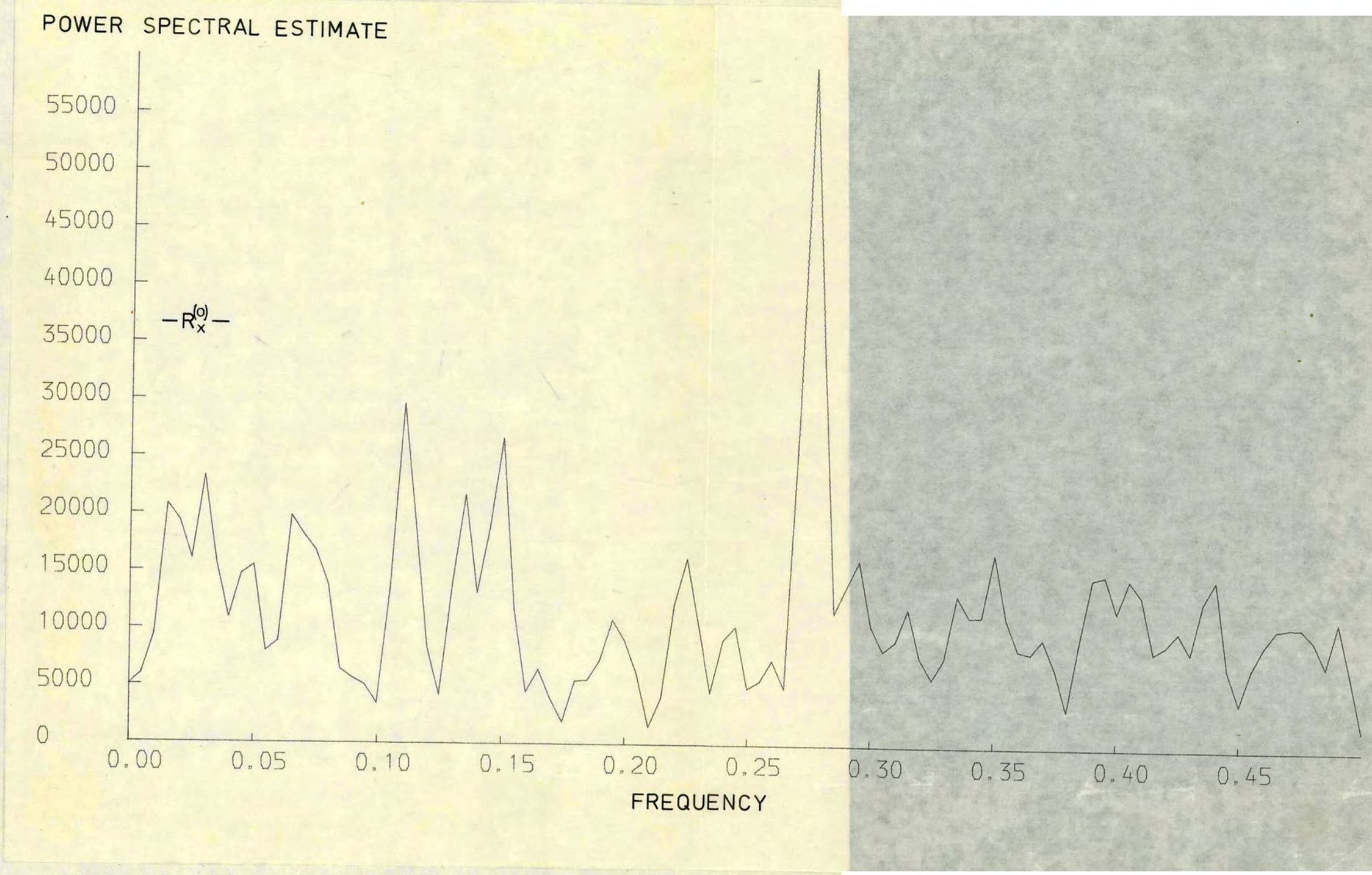

FIGURE 4.2(b). Power spectral estimates of pulse rate series computed from observations 1-300 (m=100) plotted against frequency.

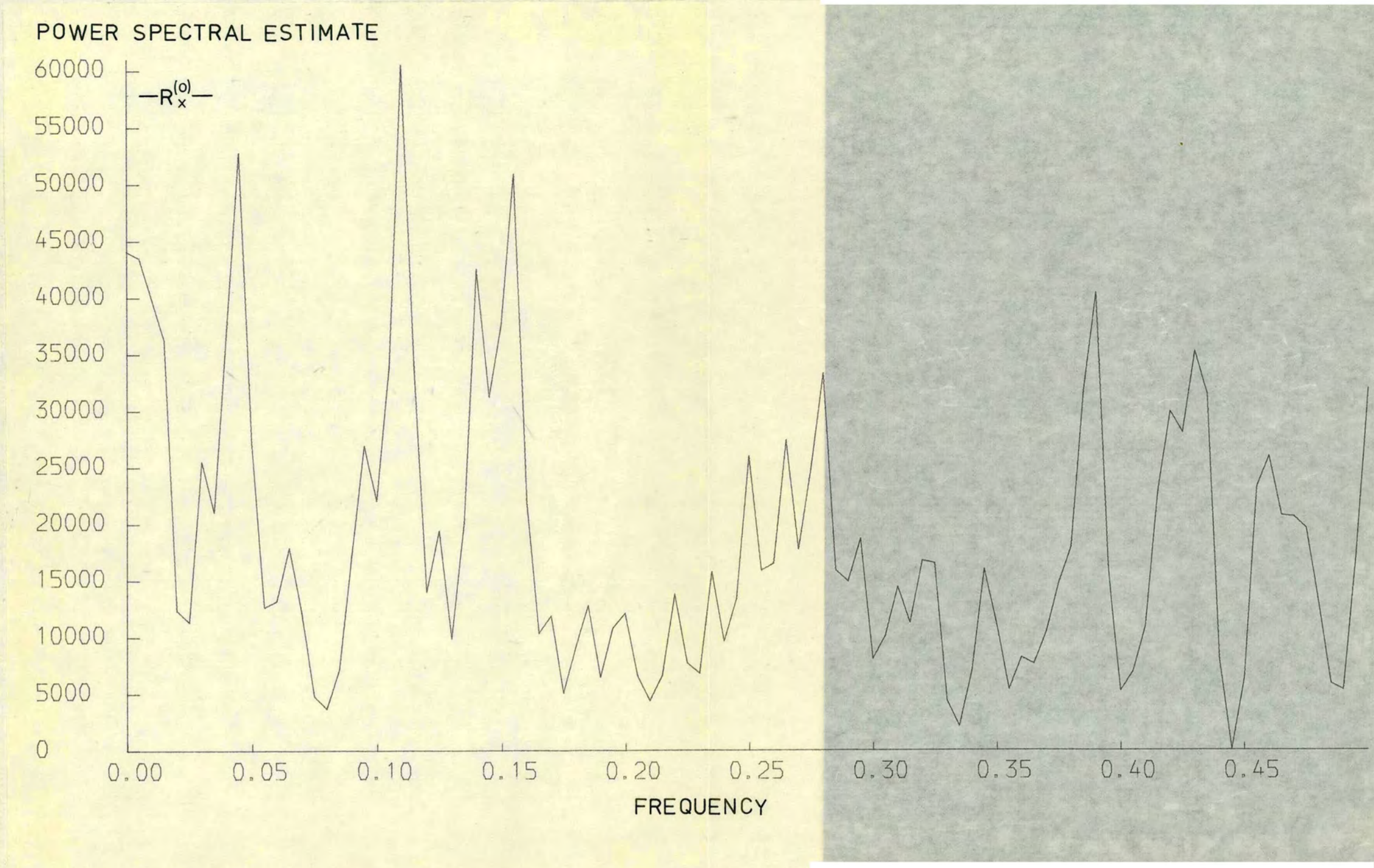

estimates for pulse rate exhibits several peaks; the highest of these is at a frequency of 0.110 c.p.s., at which the value of the spectral density is 1.05, and this peak corresponds to the peak of the blood pressure estimates at the same frequency. The pulse rate estimates also show peaks at 0.045 c.p.s., a cycle of length 22.2 seconds, which is within the range of the Mayer cycle, and 0.155 c.p.s., a cycle of length 6.5 seconds, which have spectral density values 0.91 and 0.88 respectively. There is no peak at 0.275 c.p.s., and a peak at 0.280 c.p.s. is only a minor one.

To summarize the power spectral estimates obtained from the first five minutes of the record, it was found that:

(a) there appears to be a respiratory cycle of 3.6 seconds in blood pressure which is not present in pulse rate;

(b) there is some evidence of a Mayer cycle of 22.2 seconds in the pulse rate record, but the blood pressure record shows only a relatively minor cycle of a different length;

(c) there is a common cycle of 9.1 seconds in both records for which there is no obvious physiological explanation.

Figures 4.3(a) and 4.3(b) show the graphs of the power spectral estimates for observations 301-600. The striking feature of both graphs is the high power at the origin and frequencies 0.005 c.p.s. and 0.010 c.p.s. This is an indication of some form of trend present in the input series although none was apparent from the graphs of these series. None of the peaks exhibited by the power spectral estimators for observations 1-300 are present in the estimates for observations 301-600, and the only major peak is exhibited by

FIGURE 4.3(a). Power spectral estimates of blood pressure series computed from observations 301-600 (m=100) plotted against frequency.

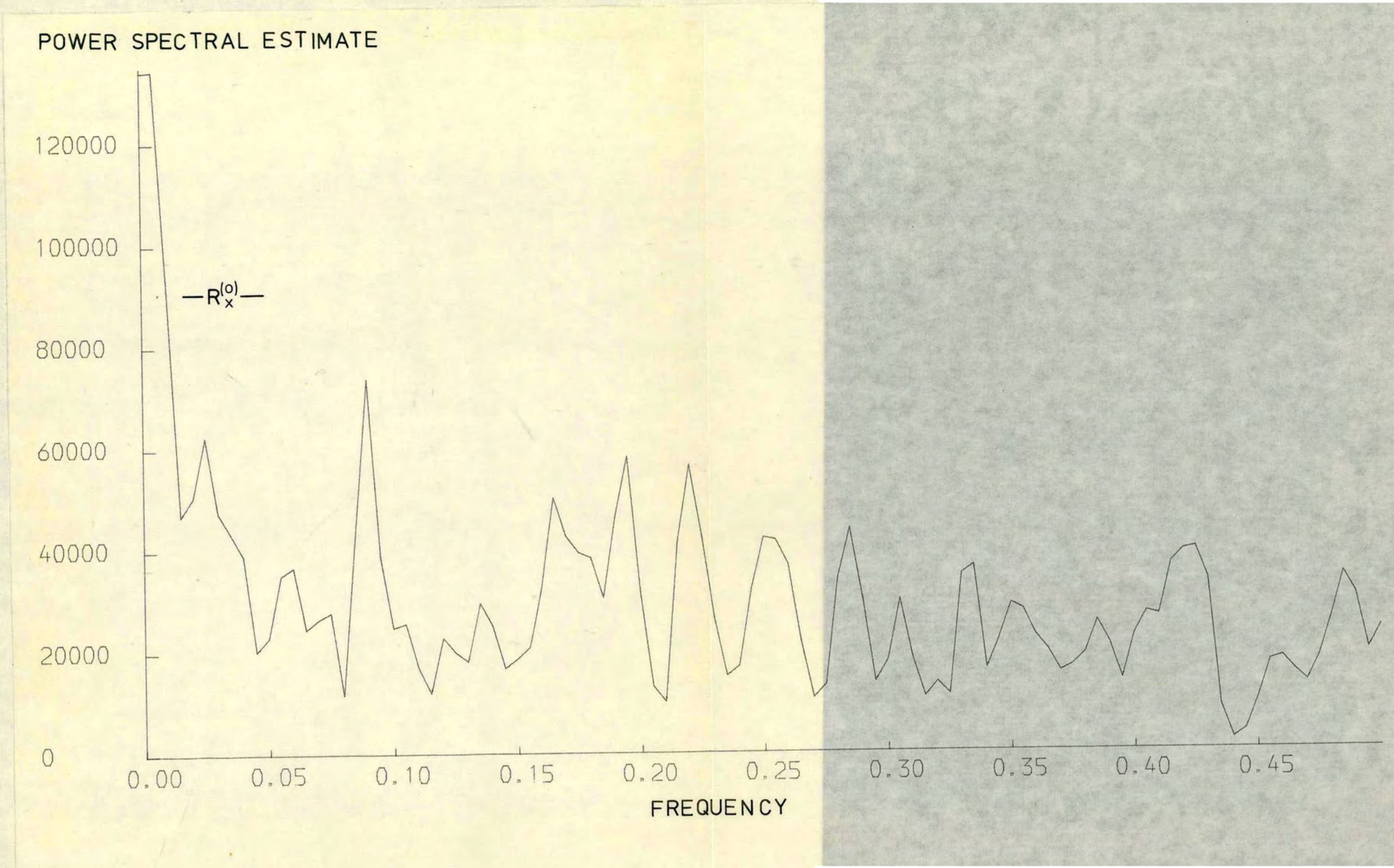

FIGURE 4.3(b). Power spectral estimates of pulse rate series computed from observations 301-600 (m=100) plotted against frequency.

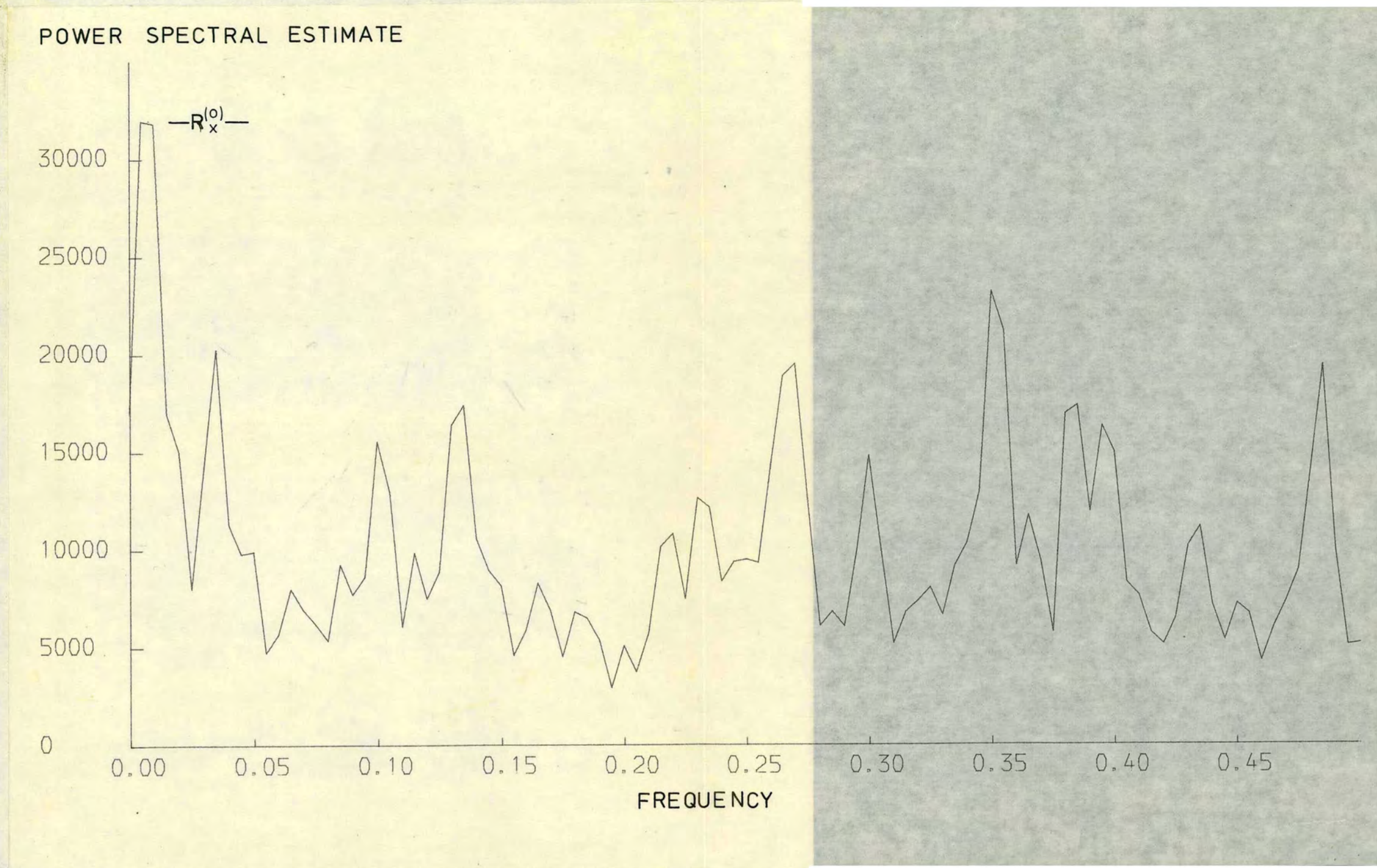

the pulse rate estimates at a frequency of 0.350 c.p.s., a cycle of length 2.9 seconds, which is likely to be a respiratory cycle.

To summarize the second five-minute period of the record it was found that both series exhibited a trend which was not formerly apparent, and that a respiratory cycle of 2.9 seconds was found in the pulse rate record which was not reflected in the blood pressure record. There was no evidence of a Mayer cycle in either record, and the behaviour of the series in this second five-minute period was in no way similar to their behaviour in the first period.

Figures 4.4(a) and 4.4(b) show the graphs of the power spectral estimates computed from observations 601-900. Once again the estimates for blood pressure show high power at the origin, indicating a trend which in this case may be caused by the fluctuation and extremity of the final 20 observations. However, if this were true one would expect the pulse rate estimates to show a similar indication of trend, but this is not the case even though the final 20 pulse rate readings seem to behave more wildly than those of the blood pressure series. The only marked peak of the power spectral estimates of the blood pressure record occurs at a frequency of 0.045 c.p.s., a peak exhibited by the pulse rate estimates of observations 1-300. The estimated spectral density at this frequency is 1.30, and the cycle length of 22.2 seconds falls within the bounds of the length of a Mayer cycle. As far as the respiratory cycle is concerned the highest value of the estimated spectral density of the blood pressure record in the range

FIGURE 4.4(a). Power spectral estimates of blood pressure series computed from observations 601-900 (m=100) plotted against frequency.

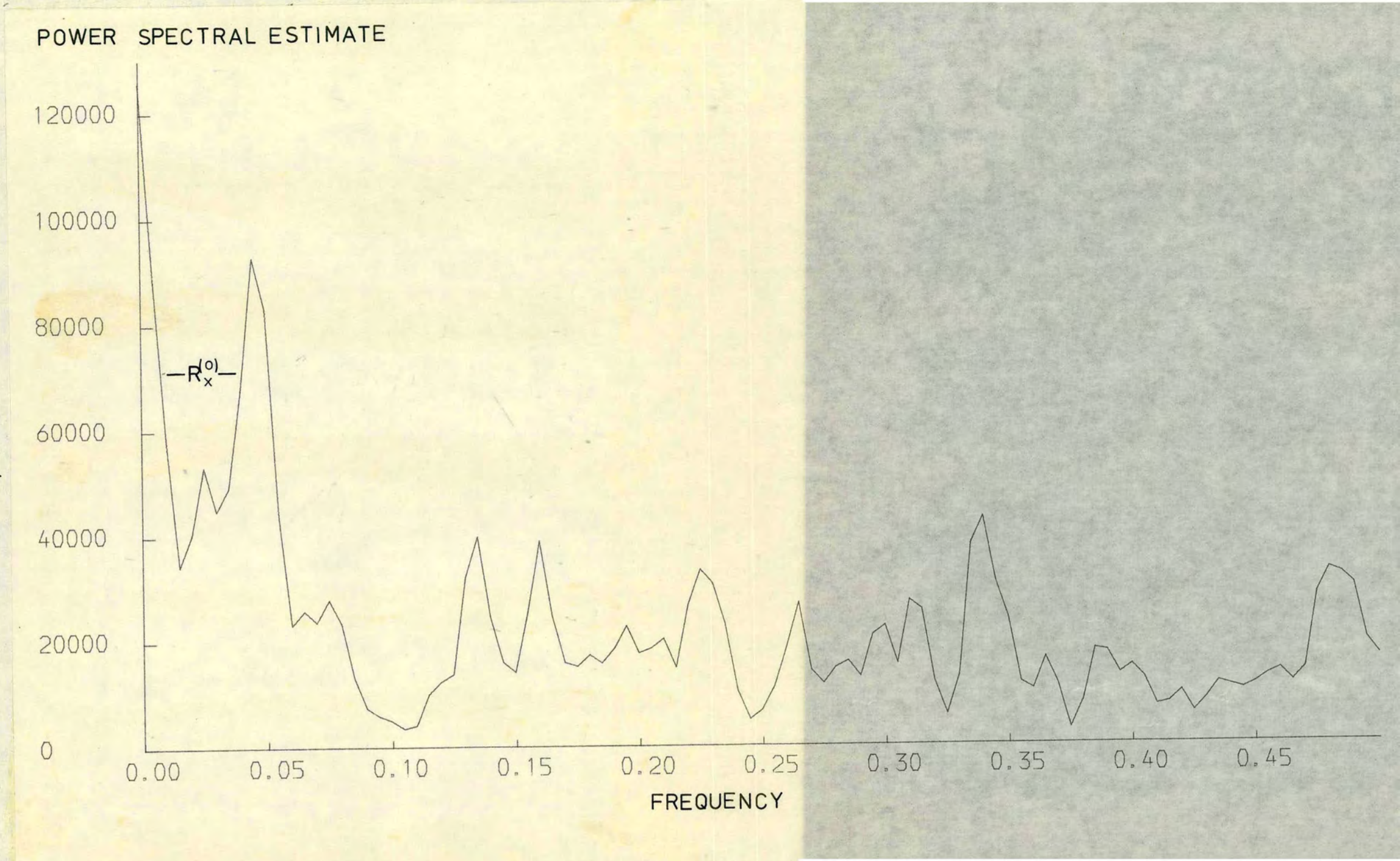

FIGURE 4.4(b). Power spectral estimates of pulse rate series computed from observations 601-900 (m=100) plotted against frequency.

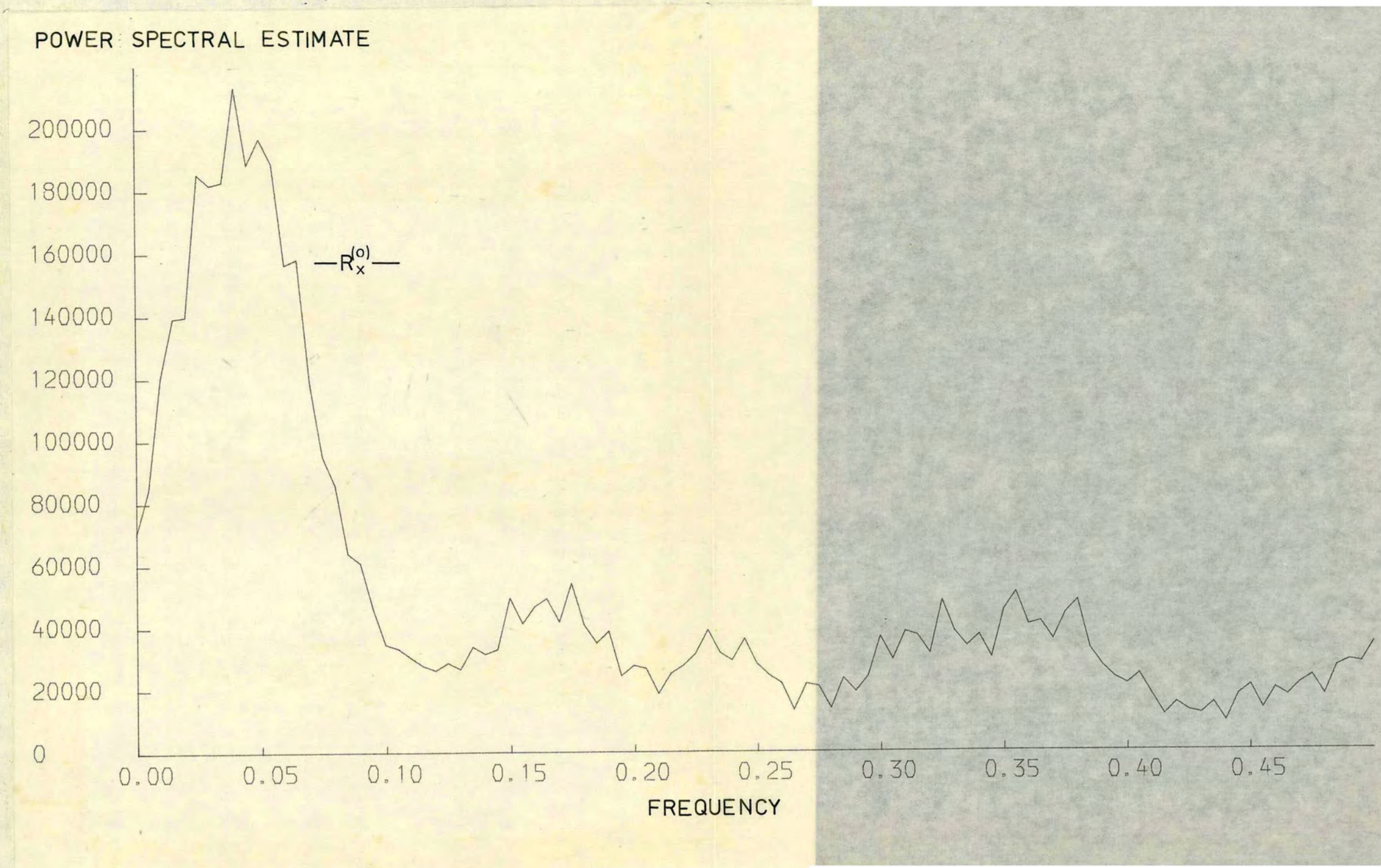

0.200-0.333 c.p.s. is 0.47 at a frequency of 0.225 c.p.s., a very minor peak. The graph of the power spectral estimates for the pulse rate record is extremely smooth with a single peak at a frequency of 0.040 c.p.s., a cycle length of 25 seconds, which has an estimated spectral density of 1.35. However the values of the estimates near this frequency are of the same order, and so this cycle could easily correspond to that present in the blood pressure observations.

The final five-minute period of the data exhibited strong evidence of a Mayer cycle in both series, at a frequency comparable with that found in the pulse rate record of observations 1-300. There was no evidence of an important respiratory cycle in either series, and there was an apparent trend in the blood pressure record which may have been caused by the final 20 observations.

Figures 4.5(a) and 4.5(b) show the graphs of the power spectral estimates of blood pressure and pulse rate respectively plotted against frequency, computed from observations 1-900 with m=199. For the blood pressure series, even though some of the apparently minor peaks have a spectral density as high as 0.9, the graph is dominated by a huge amount of power at the origin. This suggests that either the trends noted in the last ten minutes of the record have "overwhelmed" the marked periodicity of the first five minutes to produce a trend in the fifteen minute record or the behaviour of the three five minute records is not a reflection of the state of statistical equilibrium required for the assumption of stationarity to hold, i.e. that the structure of the record does depend on absolute time. The graph of the estimates also shows no marked

FIGURE 4.5(a). Power spectral estimates of blood pressure series computed from observations 1-900 (m=199) plotted against frequency.

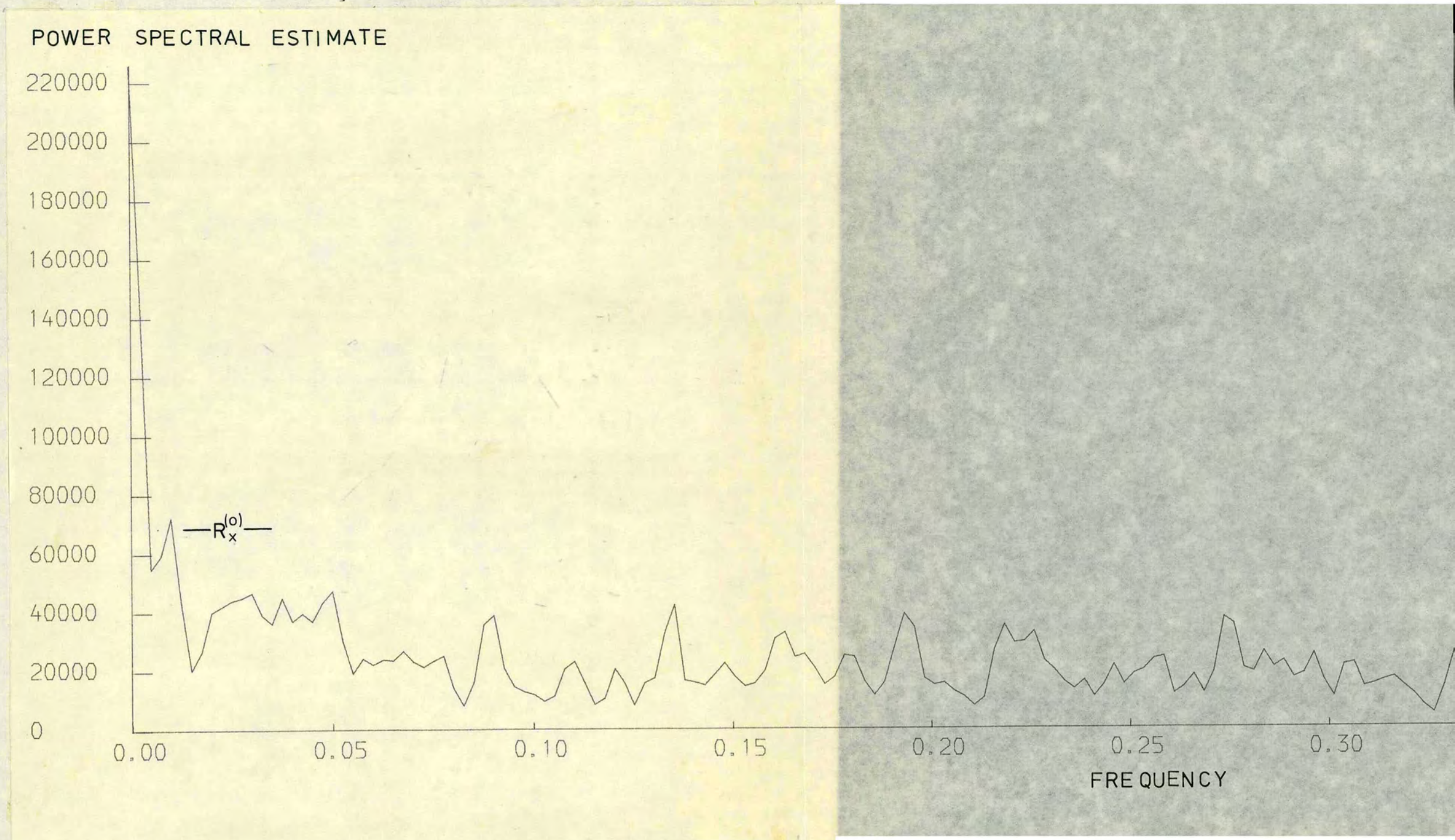

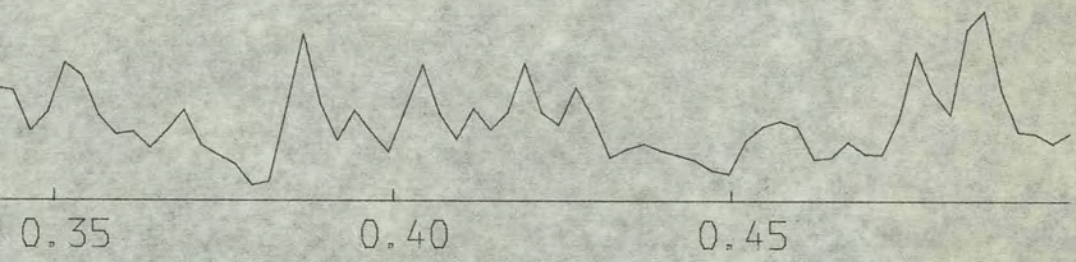
0.35
0.40
0.45

FIGURE 4.5(b). Power spectral estimates of pulse rate series computed from observations 1-900 (m=199) plotted against frequency.

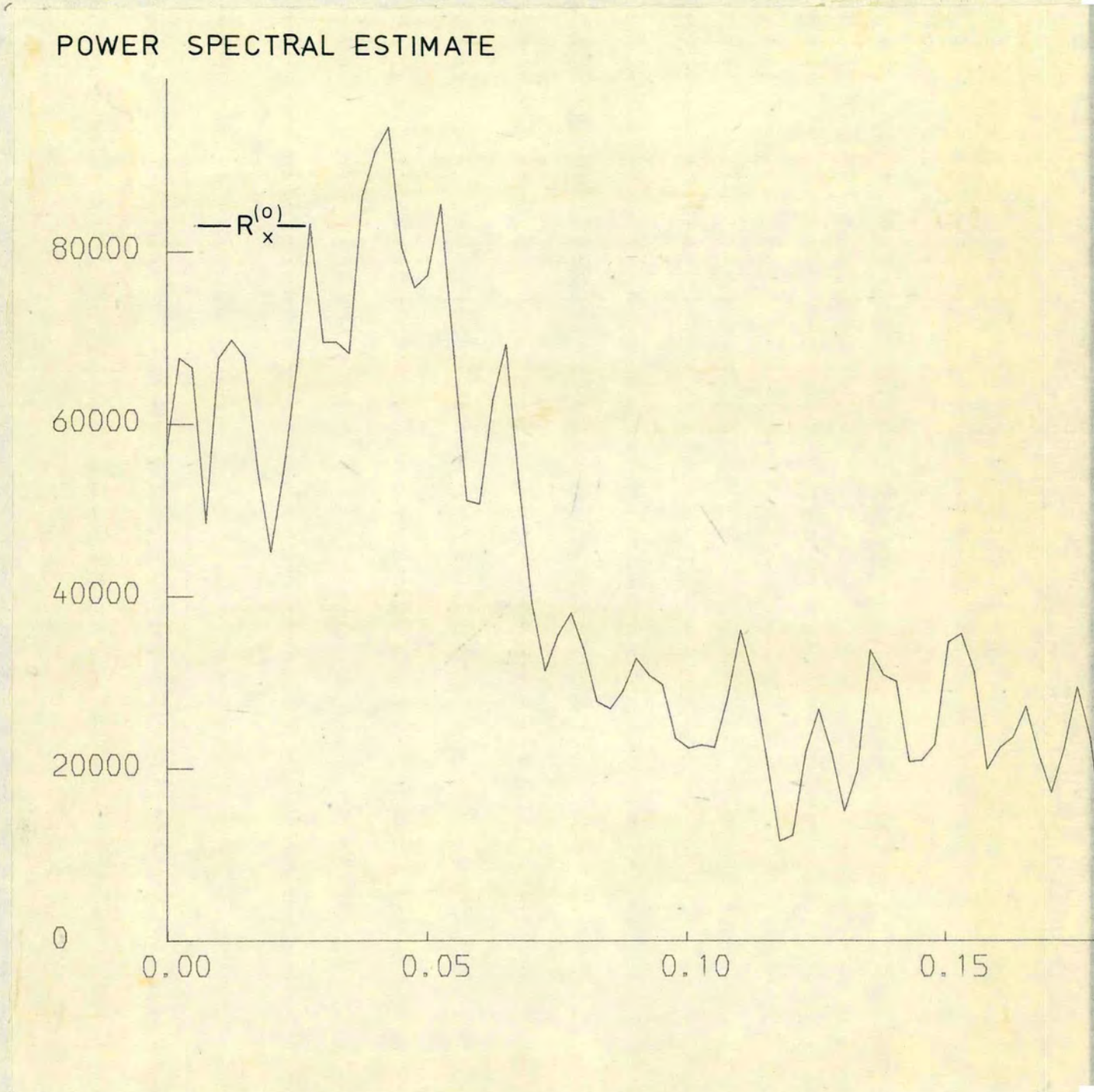

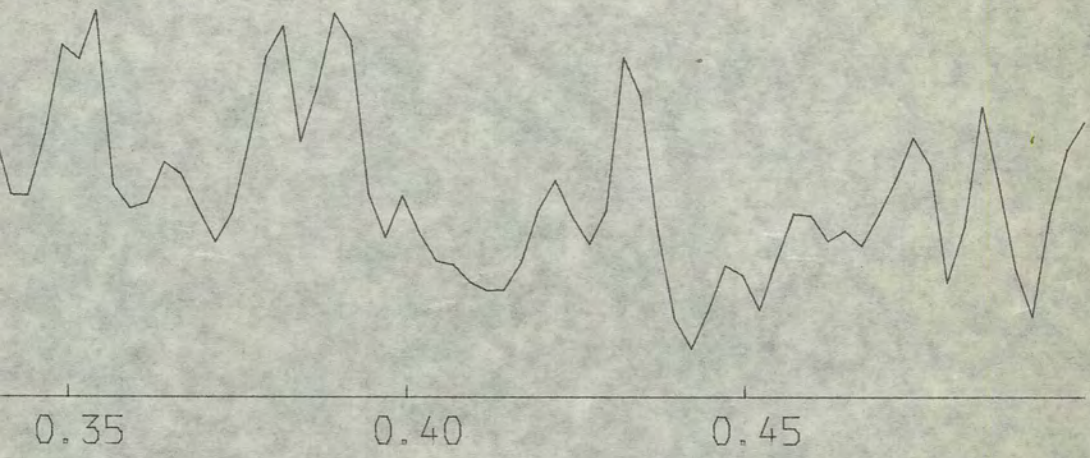
0.35
0.40
0.45

peaks in the range of either the respiratory cycle or the Mayer cycle. On the other hand the power spectral estimates of the fifteen minute pulse rate record again form a very smooth curve with a single peak at 0.043 c.p.s., a cycle length of 23.3 seconds, which has an estimated spectral density of 1.14. This would appear to support the findings of a Mayer cycle in the pulse rate record, as detected in the first and third five-minute interval. There is no evidence of a strong respiratory cycle in the pulse rate record, nor is there any indication of a trend in the series.

It did appear possible that some of the non-stationarity exhibited by the blood pressure series could have been caused by the final 20 observations, and this possibility was investigated by analysing observation 1-880 as described in Section 3.3 (run E). However it was found that the graph of the power spectral estimates for blood pressure remained unchanged in form when these last 20 observations were removed. Unfortunately the removal of these observations had a severe effect on the power spectral estimates for pulse rate, producing a graph with huge power at, and at frequencies close to, the origin and several minor peaks. The estimated spectral density at the origin was 1.03. The largest minor peaks were at frequencies 0.045 c.p.s., (cycle length 22.2 seconds, estimated spectral density 0.61), the Mayer cycle previously detected, 0.111 c.p.s., (cycle length 9.0 seconds, estimated spectral density 0.67), a cycle detected in both series during the first five minutes of the records but without any obvious physiological meaning, 0.136 c.p.s. and 0.389 c.p.s., (cycle lengths 7.3 seconds and

2.6 seconds, estimated spectral densities 0.65 and 0.66 respectively), two further cycles without obvious physiological meaning.

When observations 1-880 were analysed the power spectral estimates of both variables showed huge power at the origin, and in order to investigate whether this was due to a trend in the mean of each series the detrending option was used on these observations (run F). The program fitted a linear trend to each of the input series using standard least squares methods and then removed the trend. The linear detrender was the only detrending option available in the BMD program and was used with no great expectation of improvements in the spectral pattern. The resulting graphs of the power spectral estimates are shown in Figures 4.6(a) and 4.6(b). It can be seen from these graphs that the detrending process has had virtually no effect and that large amounts of power are still concentrated at frequencies near the origin for both series.

Finally in this section Figures 4.7(a) and 4.7(b) show the power spectral estimates for blood pressure and pulse rate respectively computed from observations 1-300 using m=100 and m=60. It can be seen that the shorter window has produced a smoother curve in each case (by reducing the variance of the estimates) but that peaks near to each other are better detected by the longer window, thus confirming the discussions on data windows in Section 3.2.3. The single marked peak of the blood pressure series, denoting a respiratory cycle, is still very much in evidence, but the secondary peak shown by the longer window at 0.110 c.p.s. is somewhat reduced by the

FIGURE 4.6(a). Power spectral estimates of blood pressure series computed from observations 1-880 (m=199) after detrending plotted against frequency.

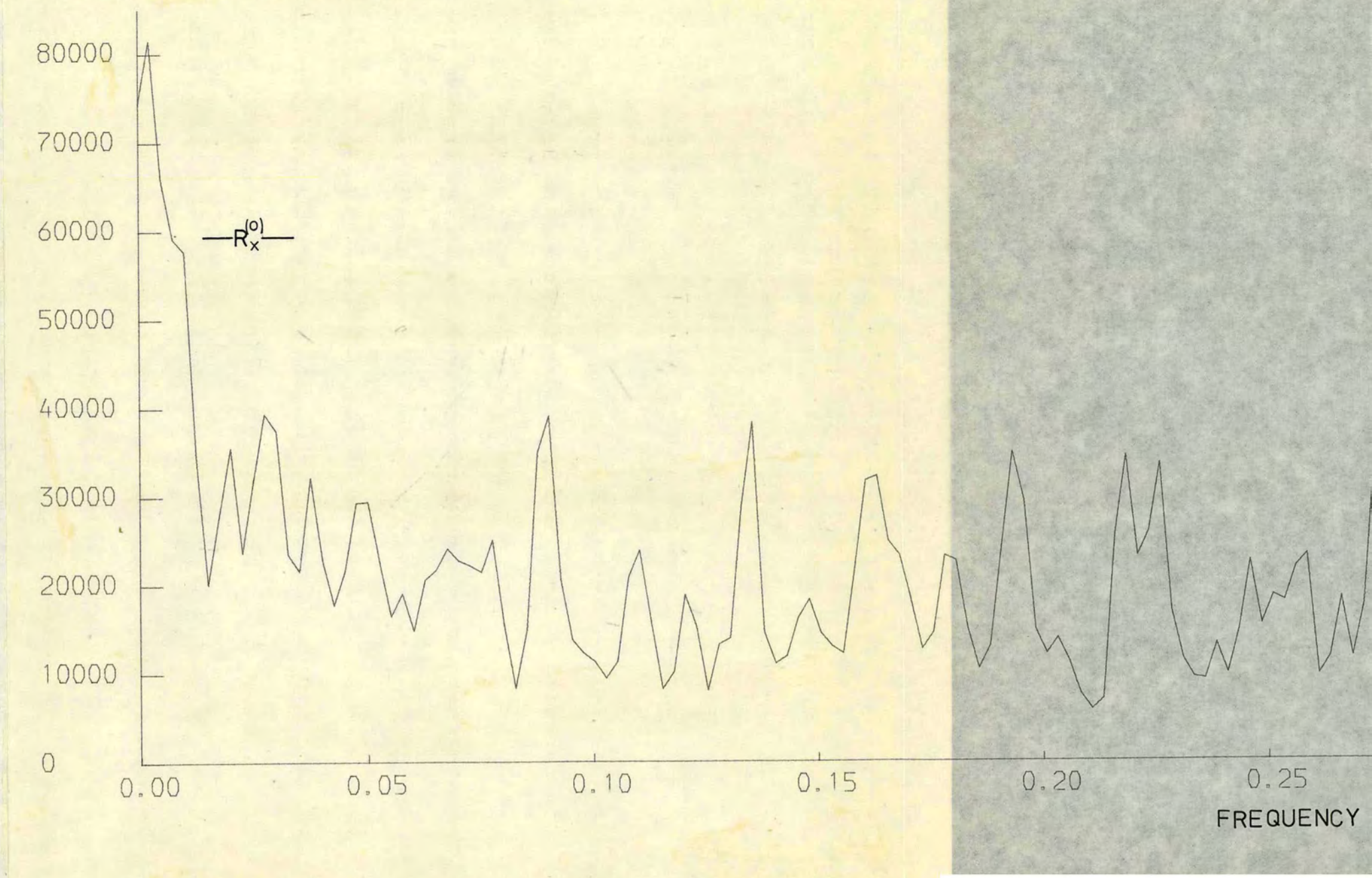

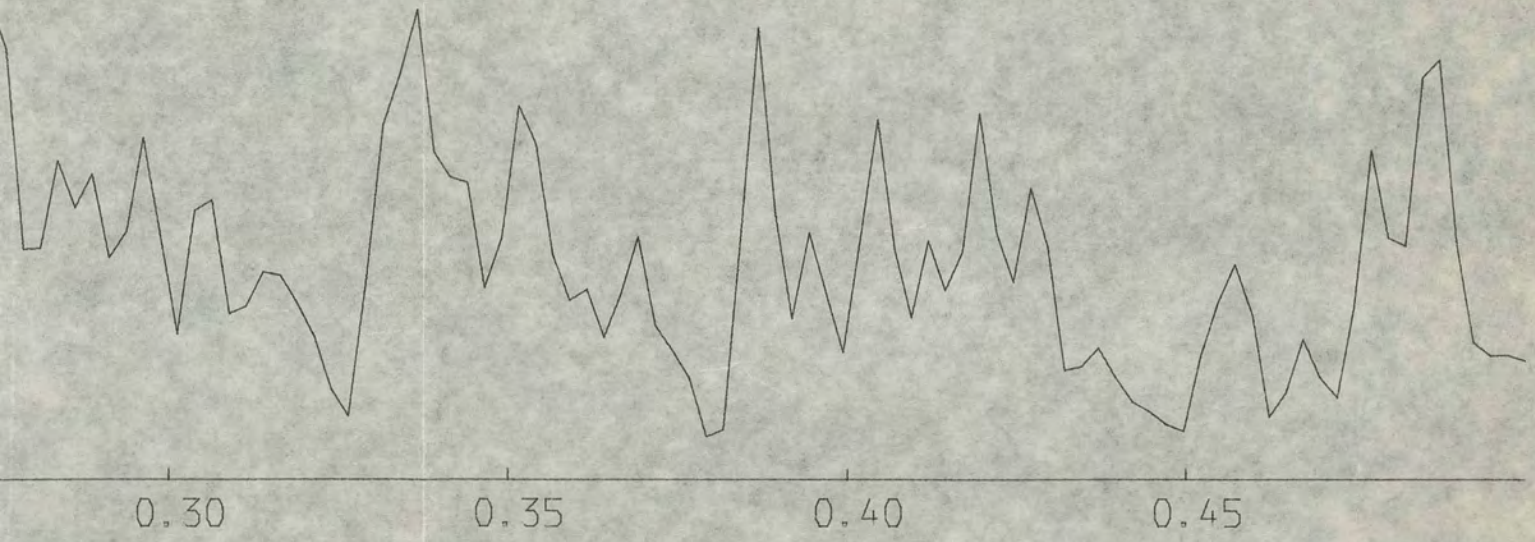
0.30
0.35
0.40
0.45

FIGURE 4.6(b). Power spectral estimates of pulse rate series computed from observations 1-880 (m=199) after detrending plotted against frequency.

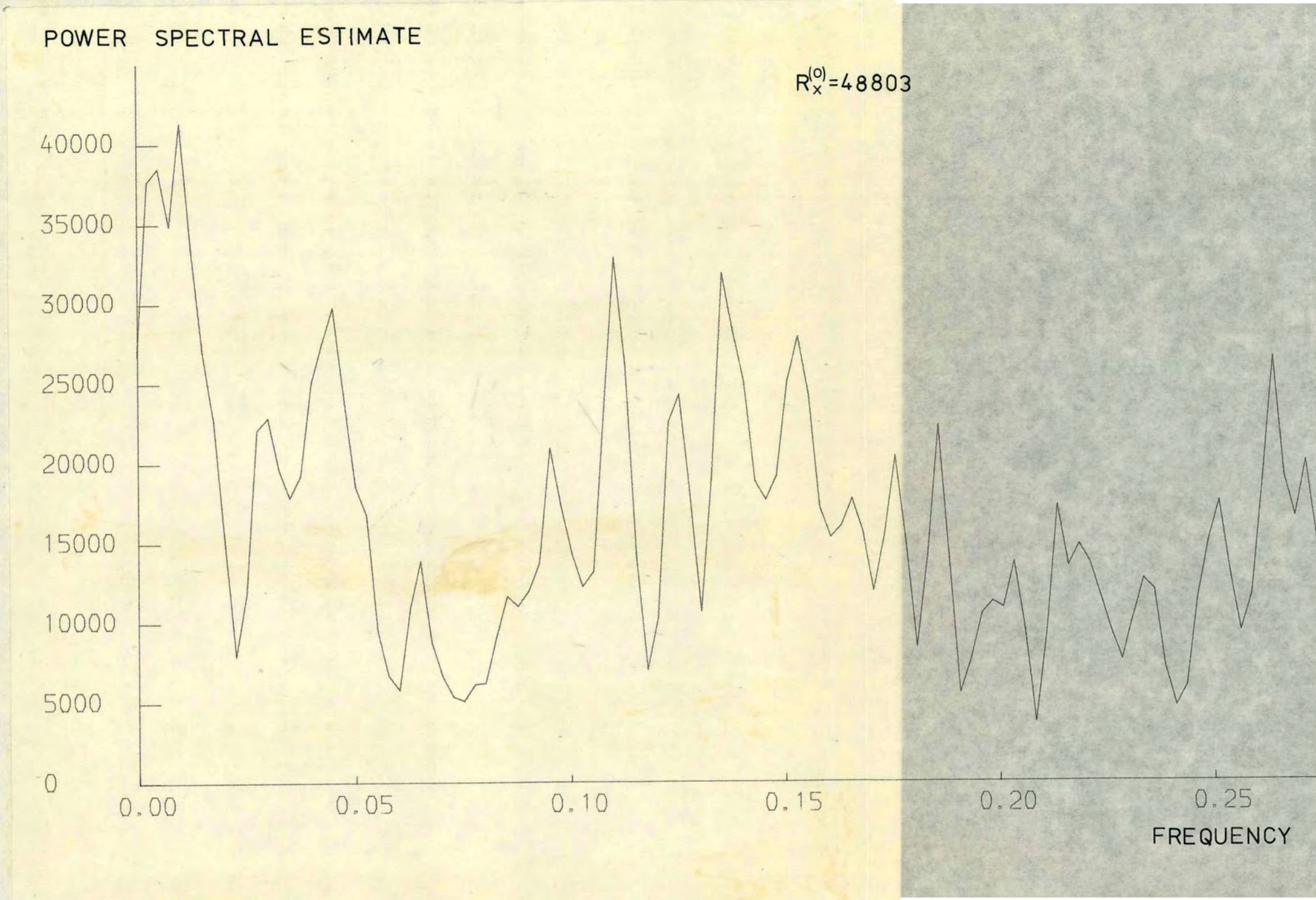

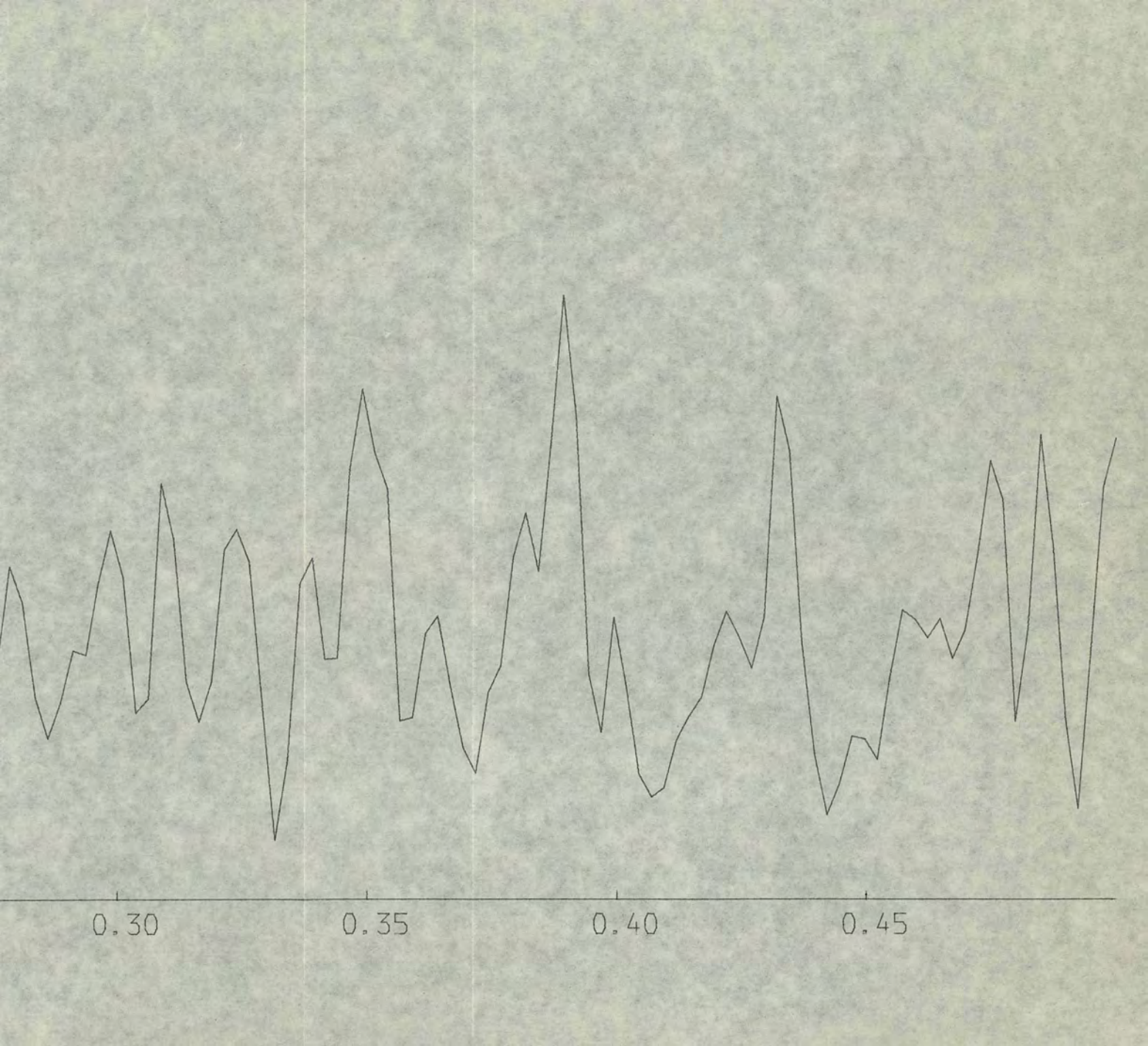
0.30
0.35
0.40
0.45

FIGURE 4.7(a). Power spectral estimates of blood pressure series computed from observations 1-300 plotted against frequency: comparison of m=100 and m=60.

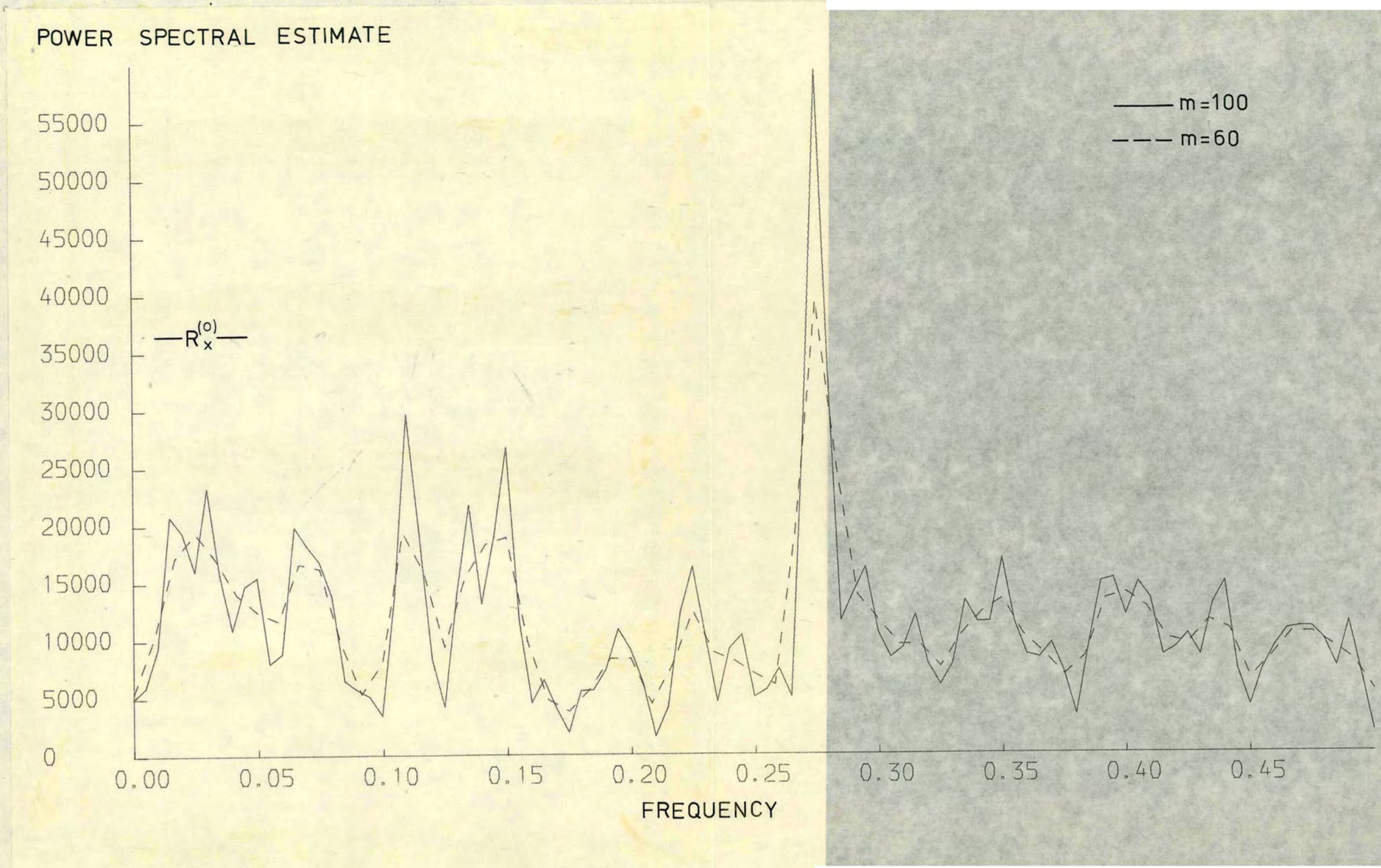

FIGURE 4.7(b). Power spectral estimates of pulse rate series computed from observations 1-300 plotted against frequency: comparison of m=100 and m=60.

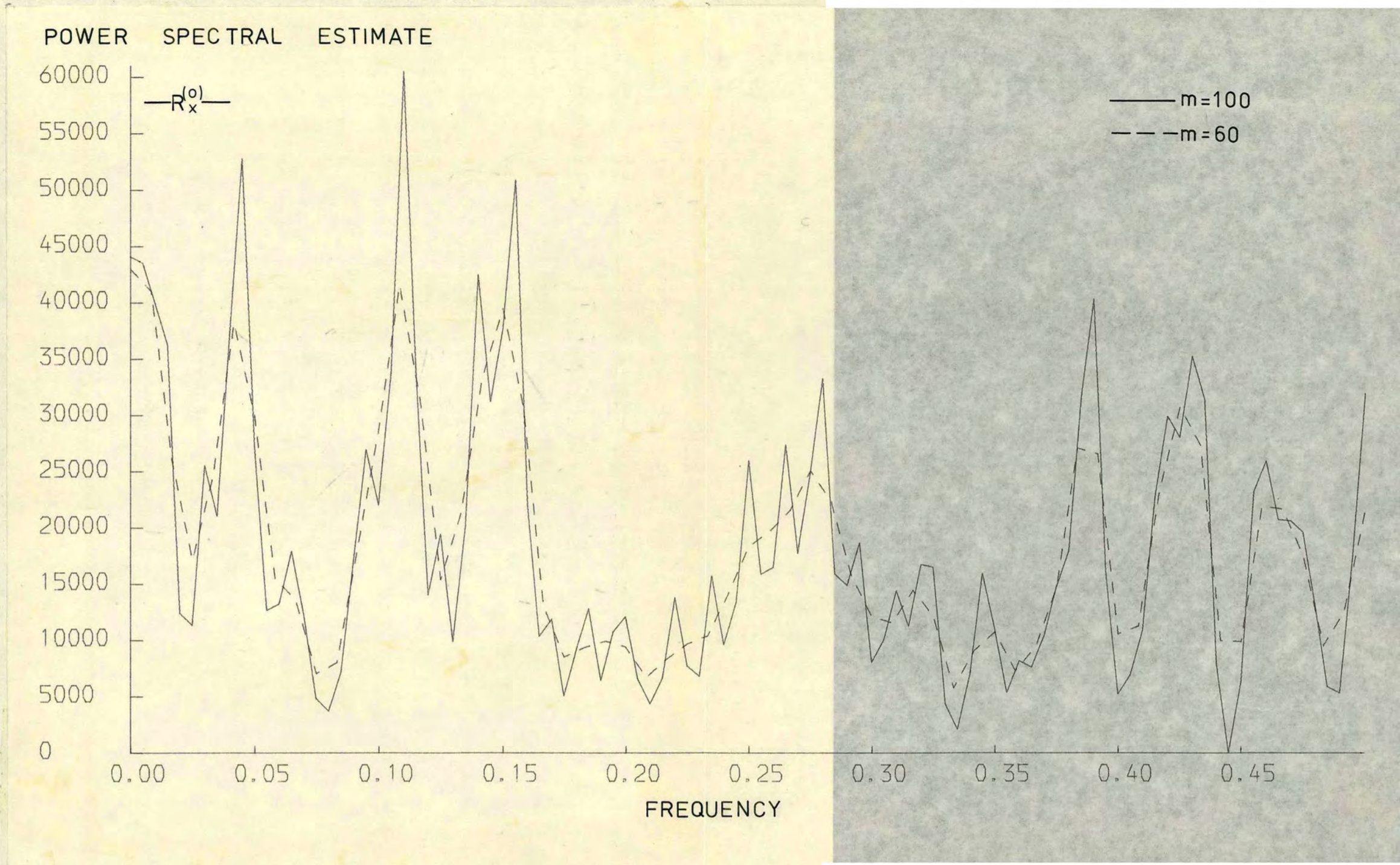

the shorter window. In the pulse rate estimates relatively more power is attributed to the origin by the shorter window, but the graph still shows several peaks at frequencies equal to or near those peaks detected by the longer window.

4.4 Cross-Covariance and Cross-Spectral Analysis

In all the analyses performed in this study there was a sizeable negative value of the cross-correlation function at zero lag, indicating that a large pulse rate reading tends to be paired with a small blood pressure observation, and vice versa. However, as in the univariate autocorrelation results, this correlation could hardly be described as strong, the largest absolute value of the cross-correlation function being 0.39 (negative) at zero lag for the series of observations 601-900. One other interesting observation made on the results of this study was that the oscillations of the cross-correlation function did not subside very quickly as $|p|$ increased.

Further interpretation of the cross-covariance function was impossible, so aspects of the relationships between the two series were investigated using the coherence squared and phase spectrum.

Figure 4.8 shows the graph of the estimated coherence squared between pulse rate and blood pressure plotted against frequency for observations 1-300. The peak at 0.445 must be ignored. The computed value of the coherence squared at this frequency was 9.84, and was therefore flagged as being erroneous due to sampling error (as described in the Appendix), but was set equal to the maximum of the remaining values for plotting purposes. However, the value of the coherence squared at 0.335 c.p.s. is 0.975, indicating that the two series are

FIGURE 4.8. The estimated coherence squared between pulse rate and blood pressure computed from observations 1-300 (m=100) plotted against frequency.

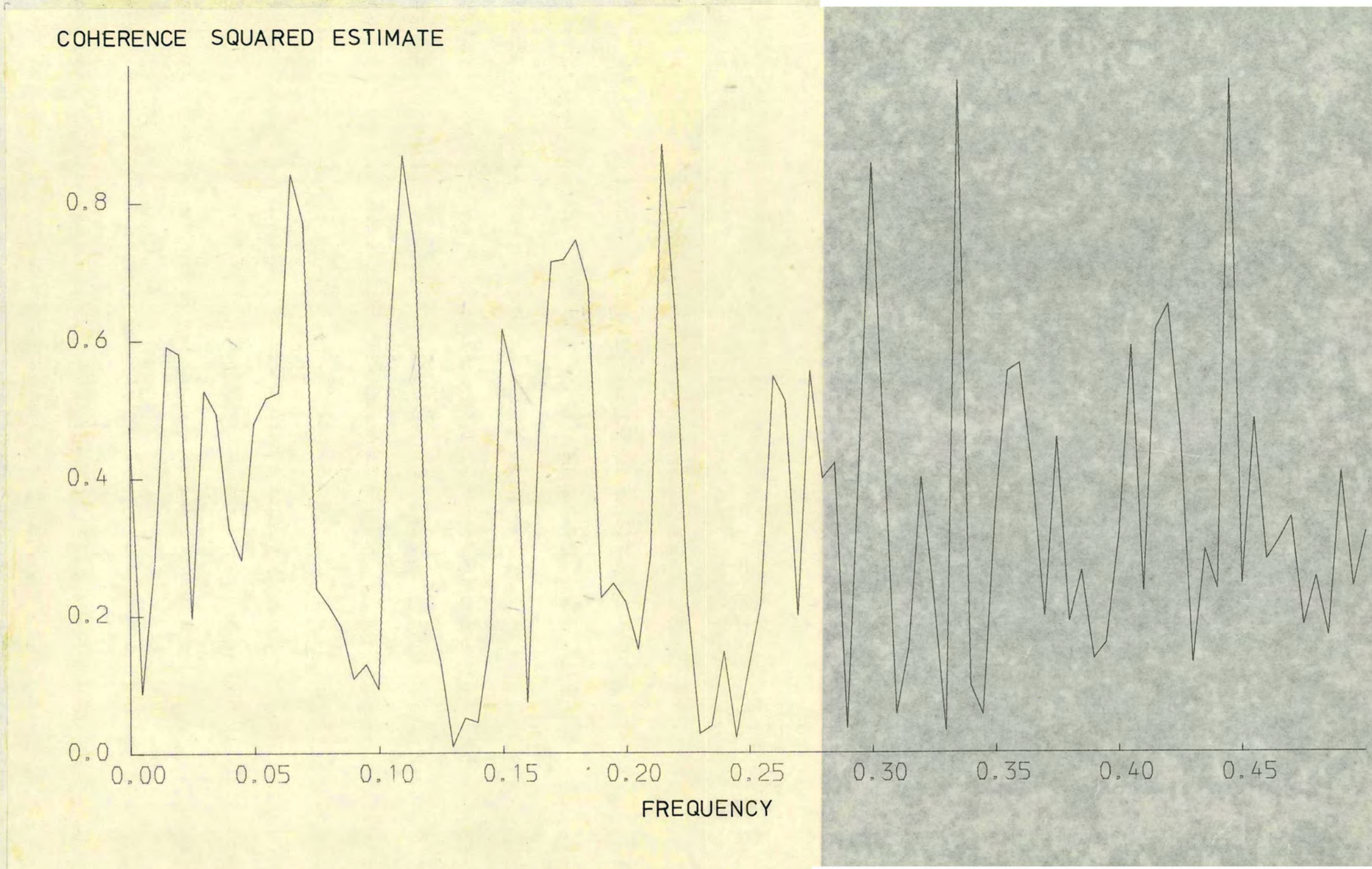

highly correlated at this frequency, which represents a cycle length of 3.0 seconds and is almost certainly a respiratory cycle. This high coherence was a little surprising since no cycle of this length in either series was indicated by the power spectral estimates computed from observations 1-300, although the blood pressure record showed a marked respiratory cycle of 3.6 seconds and the power spectral estimates for pulse rate showed a minor peak at 0.280 c.p.s., a cycle of 3.6 seconds. The phase diagram for observations 1-300 showed that at frequency 0.335 c.p.s. the pulse rate cycle led the blood pressure cycle by approximately half a second. The coherence squared estimated from the first five minutes of data possesses other peaks at 0.110 c.p.s., 0.215 c.p.s. and 0.300 c.p.s. with values 0.869, 0.883 and 0.856 respectively. The frequency 0.110 c.p.s., a cycle of length 9.1 seconds, was picked out by the power spectral estimates of both series, and the phase shift associated with this frequency is approximately π, i.e. one series leads the other by about half the cycle length.

Figure 4.9 shows the graph of the estimated coherence squared plotted against frequency for observations 301-600. It has three major peaks. The first is at 0.040 c.p.s., a cycle of length 25.0 seconds, with an estimated coherence squared value of 0.885. This cycle length falls within the bounds of the length of a Mayer cycle, but there were no indications of such a cycle in either series from the power spectral estimates. Again the phase shift is approximately π, with the blood pressure series leading the pulse rate series

FIGURE 4.9. The estimated coherence squared between pulse rate and blood pressure computed from observations 301-600 (m=100) plotted against frequency.

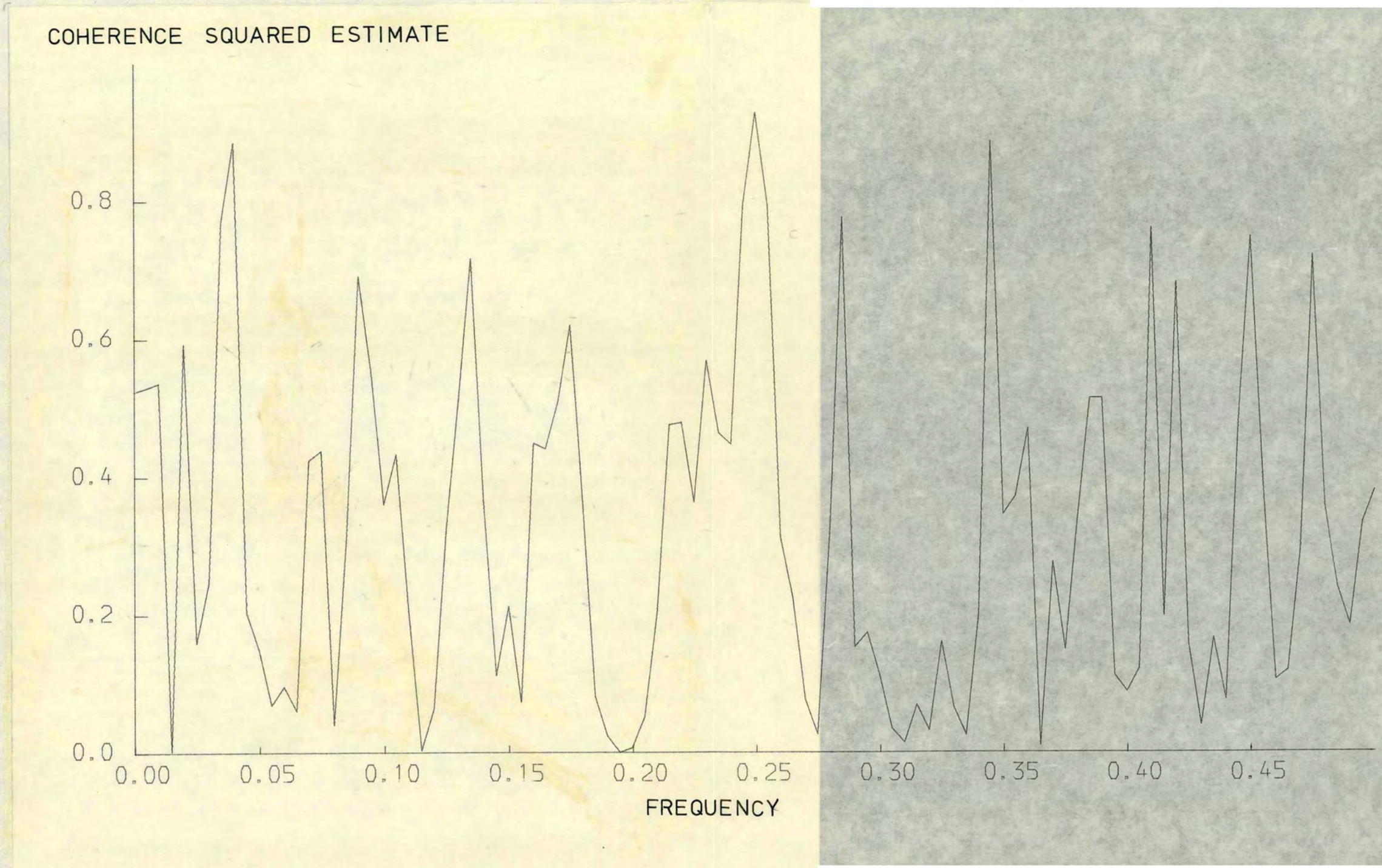

by about 11.5 seconds. The second major peak of the coherence squared estimates is at a frequency of 0.250 c.p.s., a cycle of length 4.0 seconds, with an estimated coherence squared value of 0.927. This may denote a respiratory cycle although the power spectral estimates showed no such periodicity in either series. The phase shift, once again, is approximately π, indicating that at this frequency one series leads the other by about two seconds. The third major peak, which almost corresponds to the peak found from the first five minutes of record, is at 0.345 c.p.s., a cycle of length 2.9 seconds, with coherence squared value 0.886. A cycle of this length was found in the power spectral estimates for pulse rate, so it seems more likely that this is the respiratory cycle and that the previously noted cycle of 4.0 seconds has no obvious physiological significance. At the frequency 0.345 c.p.s. it was estimated from the phase diagram that the pulse rate series is leading the blood pressure series by approximately 0.4 seconds, compared with a lead of half a second in the first five-minute interval.

Figure 4.10 shows the graph of the estimated coherence squared plotted against frequency for observations 601-900. The largest peak occurs at a frequency of 0.035 c.p.s., a cycle of length 28.6 seconds, with an estimated coherence squared value of 0.923. High coherence squared values are also found at frequencies 0.040 c.p.s. and 0.045 c.p.s., so there is strong evidence here of the presence of a Mayer cycle, particularly since both variables exhibited cycles with frequencies of this order. At frequency 0.035 c.p.s. it was

FIGURE 4.10. The estimated coherence squared between pulse rate and blood pressure computed from observations 601-900 (m=100) plotted against frequency.

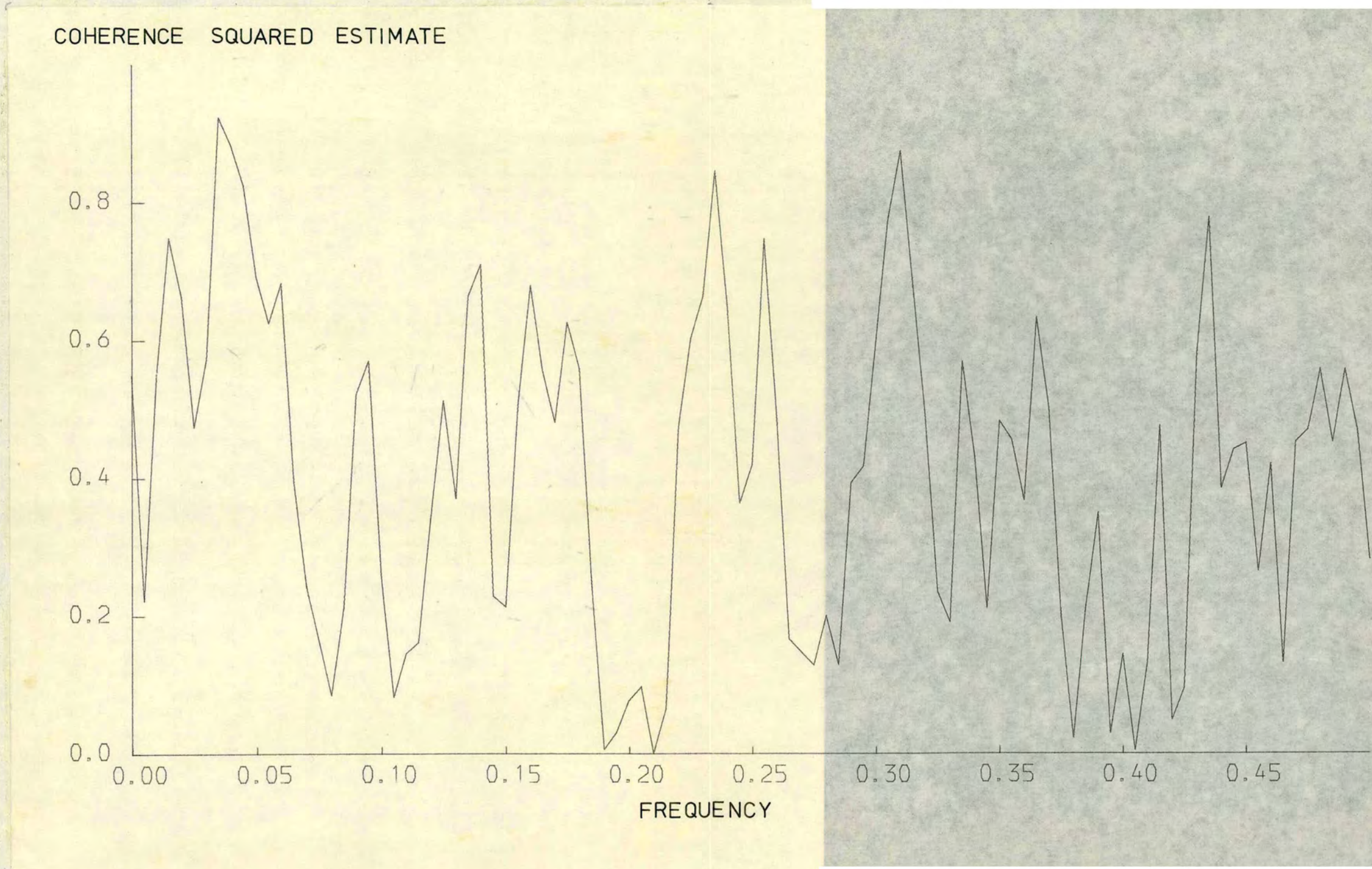

found that the blood pressure series led the pulse rate series by approximately 12 seconds, a similar situation to that recorded for the cycle of 25.0 seconds exhibited by the coherence squared estimates for observations 301-600. Returning to Figure 4.10, the second largest peak of the graph occurs at 0.310 c.p.s., a cycle of length 3.2 seconds, at which the value of the coherence squared is 0.873. This would seem to indicate a respiratory cycle, but no evidence of such was found in the power spectral estimates of either series discussed earlier. However cycles of this length have already been noted in the coherence squared estimates of the first two five-minute intervals, but in this case the pulse rate series lags the blood pressure series by approximately 1.3 seconds whereas beforehand pulse rate led blood pressure by about half a second at the frequency of the respiratory cycle.

Figure 4.11 shows the graph of the estimated coherence squared between pulse rate and blood pressure plotted against frequency for observations 1-900. A fairly marked peak at a frequency of 0.043 c.p.s. and other high values around this point confirm the evidence already gathered that there is a high correlation between the two series at a frequency in the range 0.040 c.p.s. to 0.045 c.p.s. The cycle length detected here is 23.4 seconds, the value of the coherence squared is 0.715, and the phase shift is approximately . To be more exact, the blood pressure series is leading the pulse rate series by 11.2 seconds, which agrees very closely with the results obtained from the last two five-minute periods. However it should be noted that although the power spectral

FIGURE 4.11. The estimated coherence squared between pulse rate and blood pressure computed from observations 1-900 (m=199) plotted against frequency.

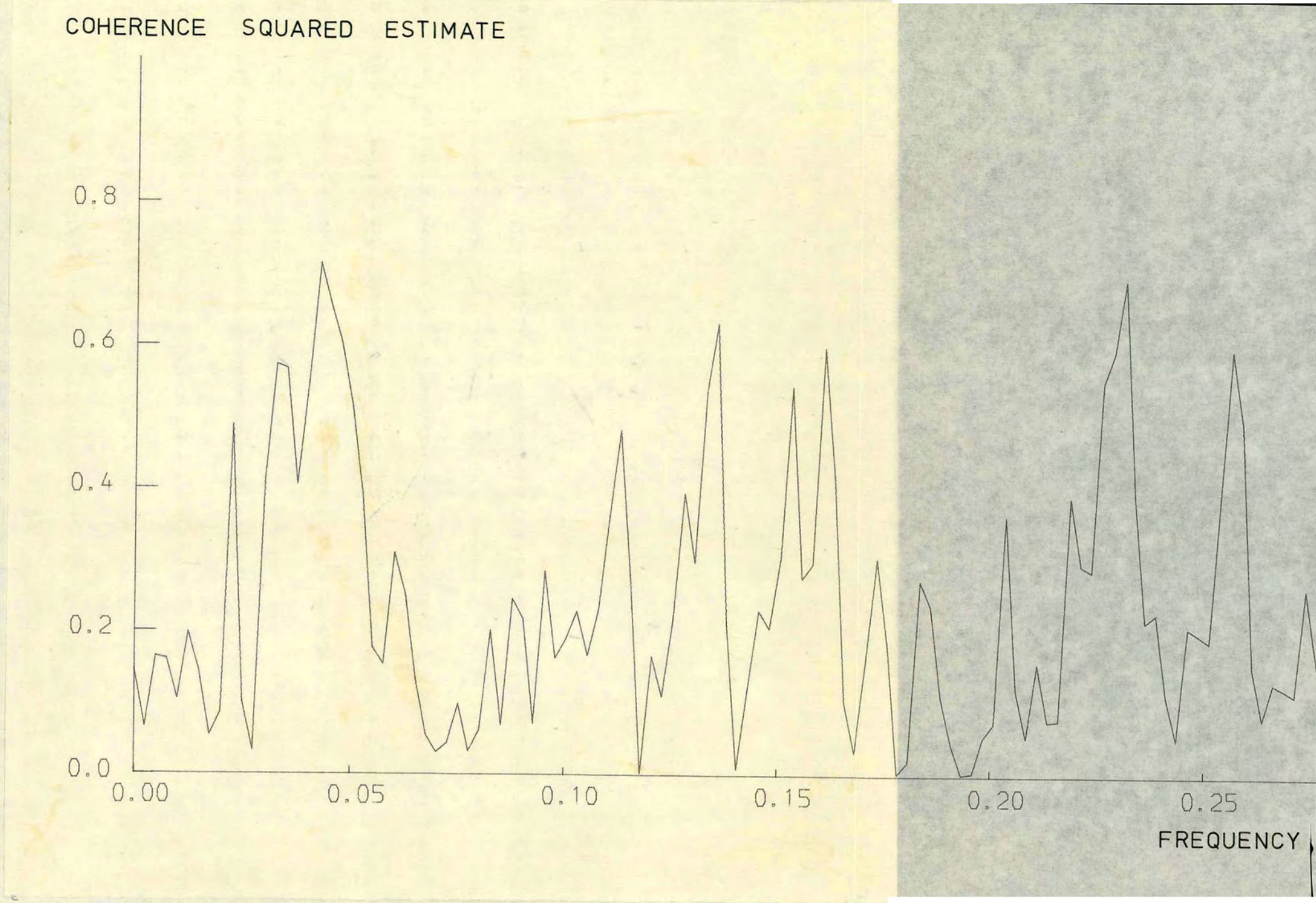

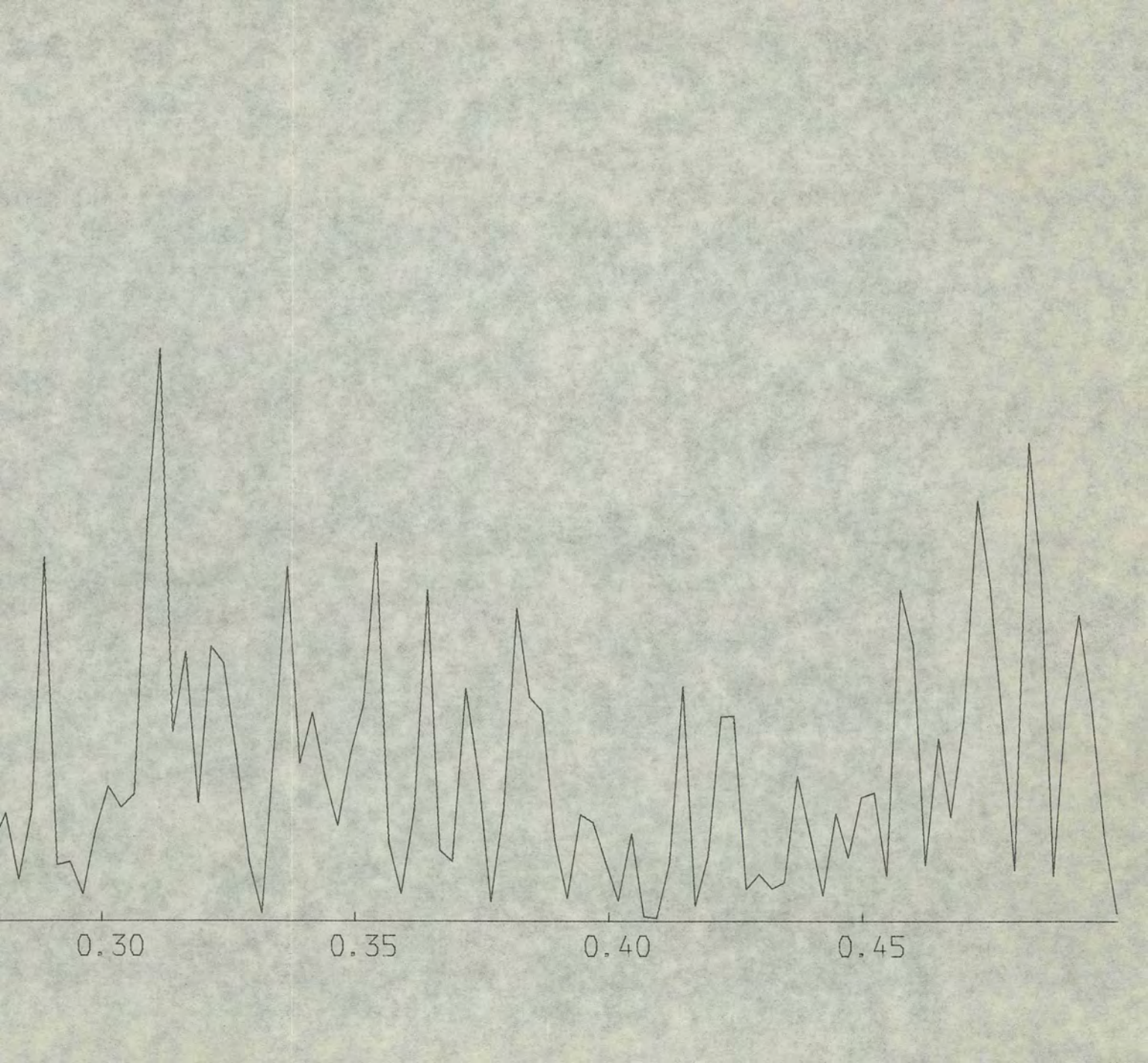
0.30
0.35
0.40
0.45

estimates of observations 1-900 showed for pulse rate a major periodic component of cycle length 23.3 seconds any such cycle which may have been present in the blood pressure record was masked by the huge power at the origin.

The second highest peak of Figure 4.11(c) occurs at 0.231 c.p.s., a cycle of length 4.3 seconds, with coherence squared value 0.695. As was the case in the second five-minute interval, where a cycle of length 4.0 had a high coherence squared value, this could be interpreted as a respiratory cycle if it were not for the presence of a third major peak, which in this instance occurs at 0.312 c.p.s., a cycle of length 3.2 seconds. Although the power spectral estimates obtained from observations 1-900 showed no evidence of a respiratory cycle in either series it has already been noted that the two series show high correlation in all three five-minute periods at a frequency close to 0.312 c.p.s. Thus it seems likely that the respiratory cycle exhibited in this data is around 3 seconds, and that the 4-second cycles have no obvious meaning. The phase diagram computed from observations 1-900 showed that at 0.312 c.p.s. the blood pressure series led the pulse rate series by 1.2 seconds, in agreement with the last five-minute interval.

The omission of the final 20 observations produced a graph of coherence squared against frequency in which all previously observed peaks were reduced, and a single marked peak introduced at a frequency of 0.256 c.p.s., a cycle of length 3.9 seconds, with an estimated coherence squared value of 0.868. At this frequency the blood pressure series was found

to lead the pulse rate series by 1.7 seconds. This is a very curious result, for which no meaningful explanation can be found.

Detrending the input series had no further effect, and the graph of the estimated coherence squared took exactly the same form as that derived from observations 1-880 without detrending.

Finally, Figure 4.12 shows the graph of the estimated coherence squared between pulse rate and blood pressure plotted against frequency for observations 1-300 using the shorter data window (m=60). It can be seen from this graph that the major peak now occurs at a frequency of 0.108 c.p.s., and that the correlation between the series in the range of the respiratory cycle is no longer high. The estimated coherence squared value is 0.711, and it was found from the phase diagram that, as before, the phase shift was approximately π.

.....

FIGURE 4.12. The estimated coherence squared between pulse rate and blood pressure computed from observations 1-300 (m=60) plotted against frequency.

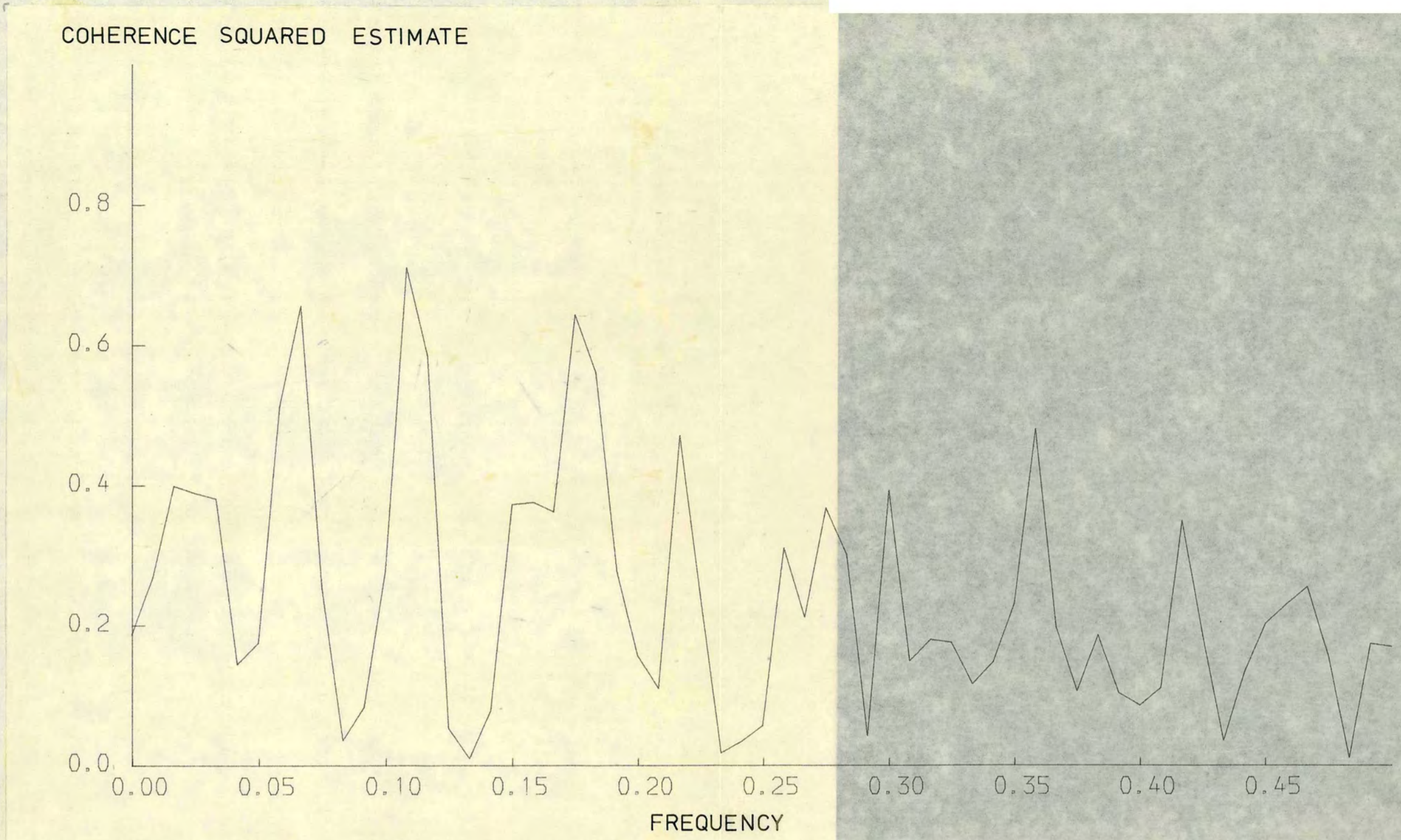

5 DISCUSSION

5.1 Extreme values

The effect that the extreme values noted in Section 4.1 have on the cyclic properties of the two variables and the phasic relationships between them is unknown, and warrants further study. It would have been instructive to analyse the series with these values omitted and replaced by a re-calculated mean in order to compare the results with those obtained in this study.

However, it has already been stated (page 22) that these extreme values are regarded as normal by the medical profession, and thus there is a need for an investigation into the frequency and occurrence of these values.

The results of Section 4.1 contain an attempt to investigate the relationship between the extremity of an observation from the mean and the presence or absence of a balancing observation extreme in the opposite direction. The staff of the Department of Physiology, Edinburgh University, have carried out work in this area using much larger sets of data, and have so far found no evidence to suggest that extremity is related to balancing.

It would have been interesting to gather more data from the records of this and other patients to investigate further the apparent trend in the blood pressure results of an unbalanced observation being more likely to lie between two and three standard deviations from the mean than a balanced observation.

It can also be noted that there were more extreme

observations in the blood pressure series than in the pulse rate series. It would have been interesting to discover whether this remained the case throughout the full eight-hour record, and if so to investigate if this had any connection with the lower-than-average short-term variability in pulse rate of this patient.

5.2 Spectral Analysis

It was noted in Section 4.3 that in no case did the autocorrelation function deviate substantially from zero after a lag of 20 seconds. This would suggest that no periodic components existed in the data but, as stated in Section 3.2.3 and as shown in the results of Section 4.3, the power spectral estimates obtained in the analyses offered a better indication of periodicity.

During the first five minutes of the record the blood pressure observations exhibited a respiratory cycle of 3.6 seconds in length, which was not markedly reflected in the pulse rate series, the pulse rate observations exhibited a Mayer cycle of 22.2 seconds in length, but the blood pressure record did not support this, and both series exhibited a cycle of 9.1 seconds in length for which there is no obvious physiological reason. The two series were highly correlated at a number of frequencies, the most prominent corresponding to a 3-second cycle, which was almost certainly due to respiration, when the pulse rate cycle was found to lead the blood pressure cycle by approximately half a second. The series were also highly correlated about the cycle of 9.1 seconds, where one series led the other by about half the cycle length.

The situation changed somewhat during the second five minute period, when both series gave indications of some form of trend which was not apparent from the data. No attempt was made to investigate or remove the trends due to lack of time. The pulse rate record did, however, exhibit a cycle of 2.9 seconds, which was taken to be a respiratory cycle, but this was not reflected in the blood pressure record. There was no evidence of a Mayer cycle in either record, but the two series were highly correlated at a cycle length of 25 seconds with the blood pressure series leading that of pulse rate by 11.5 seconds. The series were also highly correlated at frequencies 0.250 c.p.s. and 0.345 c.p.s., cycles of length 4.0 seconds and 2.9 seconds. The latter was again taken to be a respiratory cycle, and the pulse rate series led by about half a second, as in the first five minutes.

In the third five-minute period both series exhibited strong evidence of a Mayer cycle, and the series were highly correlated in this range of frequencies, with the blood pressure series leading by about 12 seconds. The series were also highly correlated at a frequency of 0.310 c.p.s., but no evidence of such a cycle was found in the power spectral estimates. There did seem to be a trend in the blood pressure series, which again was not investigated, but the final 20 observations of each series were seen to fluctuate much more wildly than the rest.

It can be seen then that these three five minute blocks have very little in common with each other. In all cases the series were highly correlated at frequencies within the range

of the respiratory cycle, but in only two out of the six cases was there evidence of an individual series exhibiting such a cycle. In the last two blocks the series were highly correlated at frequencies in the range of the Mayer cycle, but again in some cases the individual records did not exhibit this periodicity. There was also strong indication of trends in some of the records which were not investigated further. Thus it would appear that the behaviour of the two series over the fifteen-minute period is not stationary in that it is likely that the mean values and variances of the series and covariances between neighbouring values are all changing with time. This suggests that the analyses performed on the 880- or 900-observation series should be interpreted with caution.

In the analysis of the fifteen minute series it was found that the blood pressure record exhibited marked non-stationarity but that the pulse rate record exhibited a strong Mayer cycle of length 23.3 seconds, and that the two series were highly correlated at this frequency with the blood pressure series leading by 11.2 seconds. Despite the problems of non-stationarity these findings agreed remarkably well with those of the last two five-minute intervals.

It was found that the removal of the final 20 observations did not reduce the huge power at the origin of the blood pressure power spectral estimates, but introduced a similar amount of power at the origin of the pulse rate estimates. The removal of a linear trend from the records had virtually no effect.

It was stated in the introduction (page 1) that the short-term variability of the pulse rate record of this patient was

lower than average, and this fact could partly explain why strong respiratory cycles were rarely found in the pulse rate observations, but the two series were almost always highly correlated at frequencies in the range of the respiratory cycle.

In all the analyses of five-minute records and in the analysis of the fifteen-minute record there was a high coherence between the two series at a certain frequency where the phase shift was almost π (i.e. one series led the other by about half the cycle length). This could account for the considerable negative cross-correlations at zero lag, noted in Section 4.4.

5.3 Other considerations

In this study a great deal was learned about the problems of analysing data of this kind. The occurrence of extreme observations in the records which are nevertheless quite natural phenomena has already been discussed in Section 5.1.

Much more work needs to be done in investigating the presence of trends in the data. Tests for trends should be performed before spectral analysis is carried out, but even more essential is the need for the identification of the non-stationary components in the data and an attempt to discover physiological reasons for them.

In any further study of this type it would be worthwhile to take much greater care in estimating the power spectrum and cross-spectrum than is allowed by the BMD program. The choice of width and shape of the data window and the smoothing pro-

cedure should be made after much more detailed consideration of bias and variance of the spectral estimators. In this study a comparison was attempted between the maximum lag m=100 and m=60 on the first 300 observations, and the differences noted in the results, although relatively small, were a little disturbing. It can be noted that all graphs of power spectral estimates against frequency were very irregular even after smoothing, but "hamming" was the only smoothing procedure available in the BMD program. It would be worthwhile to experiment with different data windows and smoothing procedures and to use the "window closing" and "window carpentry" techniques described in Jenkins and Watts (pp280-3).

One way of removing the dominance of high power at the origin of the graph of power spectral estimates is to filter off the non-stationary low-frequency components and perform a spectral analysis on the residual series. It would have been useful in this study to have analysed the series of first-differences

$$Z_i = X_{i+1} - X_i \ , \quad i=1,2,....n-1 \ ,$$

in order to reduce the effect of high power at low frequencies and highlight the behaviour of the power spectral estimates at high frequencies. Unfortunately the prewhitening step available in the BMD program, namely

$$Z_i = X_{i+1} - CX_i \ , \quad i=1,2,....n-1 \ ,$$

only permits the use of values of C such that $|C|<1$ and, if used, prohibits the computation of the cross-spectrum.

.....

6 FINAL CONCLUSIONS

The overwhelming conclusion to be made from this study is that the records of both series are not stationary, which was a little surprising since the patient was completely immobile and in a stable clinical condition. This state of non-equilibrium can only increase the difficulties in detecting normal patterns in the two physiological variables.

However there was evidence of a respiratory cycle and a Mayer cycle present in both series. Where the Mayer cycle was found its length was between 20 and 25 seconds, and the two series were highly correlated with blood pressure leading pulse rate by about 11 seconds. The respiratory cycle was between 3 and 3.5 seconds in length, but the phase shift between the two series was not always the same. When efforts were made to remove possible sources of trend in the data these cycles disappeared.

REFERENCES

ANDERSON, T.W.(1958). The Statistical Analysis of Time Series. New York: Wiley.

DIXON, W.J.(Ed.)(1967). BMD Biomedical Computer Programs. University of California Publications in Automatic Computation No. 2. University of California Press.

HEYMANS, C. and NEIL, E.(1958). Reflexogenic Areas of the Cardiovascular System. London: Churchill.

JENKINS, G.M. and WATTS, D.G.(1968). Spectral Analysis and its Applications. San Francisco: Holden Day.

MAYER, S.(1876). Studien zur Physiologie des Herzens und der Blutgefässe: IV. Sber. Akad. Wiss. Wien, 73, 85-108.

MAYER, S.(1877). Studien zur Physiologie des Herzens und der Blutgefässe: V. Sber. Akad. Wiss. Wien, 74, 281-307.

SCHWEITZER, A.(1945). Rhythmical fluctuations of the arterial blood pressure. J.Physiol., 104, 25P.

TAYLOR, D.E.M.(1971). Computer-assisted patient monitor systems. Biomed. Eng., 6, 560-66 and 573.

TAYLOR, D.E.M., WHAMOND, J.S., HITCHINGS, D.J., HULLIGER, M. and BEGG, D.(1974). Short-term variability of pulse rate and blood pressure in cardiac surgery patients. Cardiovasc. Res. (In press).

TAYLOR, D.E.M. and associates. Unpublished data.

APPENDIX

Reproduced from Dixon (1967)

Biomedical Computer Programs. Class T - Time Series Analysis.

BMD 02T Autocovariance and Power Spectral Analysis.

1. General Description.

   a. This program computes the autocovariance, power spectrum, cross-covariance, cross-spectrum, transfer function, and coherence function of time series.

   b. Output from this program includes

      (1) Input data printed and plotted.

      (2) Autocovariance printed and plotted.

      (3) Power spectral estimates (power spectrum) printed and plotted.

      The estimates are checked for negative powers. If any occur, they are flagged, set equal to zero for future calculations, and set equal to the maximum value of the estimates for plotting purposes.

      (4) Cross-covariance of two time series printed and plotted.

      (5) Cross-spectrum of two time series printed and plotted.

      (6) Phase shift between two time series printed and plotted.

      (7) Coherence function of two time series printed and plotted.

      This function is checked to see if any values are greater than 1. If so, they are flagged as

being erroneous due to sampling error and set equal to the maximum value of the remaining functions for plotting purposes.

(8) Transfer function of two time series printed and plotted.

If any power spectral estimate was negative or zero, the corresponding transfer function of that series and the coherence function at that lag cannot be computed. These are so indicated on the output and, for plotting purposes, are set equal to the maximum value of the remaining function values.

c. Limitations per problem:

(Only limitations applicable to this study are quoted.)

(1) n, number of discrete data points per series ($1 \leq n \leq 1000$).

(2) m, number of lags ($1 \leq m \leq 199$).

d. A simple prewhitening transformation in the form of a moving linear combination $W_t = X_{t+1} - CX_t$ is optional. C is a constant supplied by the user ($|C| < 1.0$). The final spectra are then recoloured. Prewhitening cannot be used when the cross-spectrum is to be obtained.

e. The program allows detrending of the input series as an option.

2. Computational procedure.

Symbols Used.

X'_i i^{th} value of discrete, equi-spaced time series X(t).

X_i i^{th} value of time series X(t) after subtracting mean.

Y_i i^{th} value of time series Y(t) after subtracting mean.

Z_i i^{th} value of time series after prewhitening.

p Lag.

C Constant value ($|C|<1.0$) provided by user.

n Number of discrete data points.

m Maximum lag.

Δt Constant time interval.

$R_x^{(p)}$ Autocovariance of series X at lag p, ($R_x^{(p)} = R_x(p\Delta t)$).

$A_x^{(p)}$ Autocovariance of series X after detrending at lag p.

$P_x^{(h)}$ Power spectral estimate of series X at frequency $\frac{h\pi}{m\Delta t}$,

$$\left[P_x^{(h)} = P_x\left(\frac{h\pi}{m\Delta t}\right) \right].$$

$SP_x^{(h)}$ Smoothed power spectral estimate of series X at frequency $\frac{h\pi}{m\Delta t}$.

$RSP_x^{(h)}$ Power spectral estimate of series X at frequency $\frac{h\pi}{m\Delta t}$ after recolouring.

$R_{xy}^{(p)}$ Cross-covariance between series X and Y at lag p.

$A_{xy}^{(p)}$ Cross-covariance between series X and Y after detrending at lag p.

$P_{xy}^{(h)}$ Cross-power spectral estimate at frequency $\frac{h\pi}{m\Delta t}$.

$C_{xy}^{(h)}$ Cospectrum, the real part of $P_{xy}^{(h)}$ at frequency $\frac{h\pi}{m\Delta t}$.

$Q_{xy}^{(h)}$ Quadrature spectrum, the imaginary part of $R_{xy}^{(h)}$ at frequency $\frac{h\pi}{m\Delta t}$.

$SC_{xy}^{(h)}$ Smoothed cospectrum at frequency $\frac{h\pi}{m\Delta t}$.

$SQ_{xy}^{(h)}$ Smoothed quadrature spectrum at frequency $\frac{h\pi}{m\Delta t}$.

$AM_{xy}^{(h)}$ Amplitude of cross-spectrum at frequency $\frac{h\pi}{m\Delta t}$.

$PHAS_{xy}^{(h)}$ Phase of cross-spectrum at frequency $\frac{h\pi}{m\Delta t}$.

$T_{xy}^{(h)}$ Transfer function at frequency $\frac{h\pi}{m\Delta t}$.

$TAM_{xy}^{(h)}$ Amplitude of transfer function at frequency $\frac{h\pi}{m\Delta t}$.

$COSQ_{xy}^{(h)}$ Coherence square at frequency $\frac{h\pi}{m\Delta t}$.

Step 1. The mean of the data is first calculated and subtracted from each value of X'.

$$m_x = \frac{1}{n}\sum_{i=1}^{n} X_i'$$

$$X_i = X_i' - m_x, \quad i = 1,2,\ldots,n.$$

This is not done if the series is to be detrended.

Step 2. (optional). One method of prewhitening the input data is by the following moving linear combination:

$$Z_i = X_{i+1} - CX_i, \quad i=1,2,\ldots,n-1.$$

C is a value supplied by the user ($|C|<1.0$).

Step 3. The autocovariance is then computed.

$$R_x^{(p)} = \frac{1}{n-p}\sum_{q=1}^{n-p} X_q X_{q+p}, \quad p=0,1,2,\ldots,m.$$

$$R_x^{(p)} = R_x(p\Delta t).$$

Step 4. (optional) If the series is to be detrended, a least squares fitting method is used:

$$A_x^{(p)} = R_x^{(p)} - \beta - \alpha i, \quad i=0,1,\ldots,n-1,$$

where

$$\alpha = \sum_{i=0}^{n} x_i(2i-n+1)/(((n-1)n(n+1))/6)$$

and

$$\beta = \bar{x} - \alpha(n-1)/2, \text{ where } \bar{x} \text{ is the mean.}$$

Step 5. The raw estimate of the power spectrum is obtained by

$$P_x^{(h)} = \frac{2\Delta t}{\pi}\sum_{p=0}^{m}\varepsilon_p R_x^{(p)} \cos\frac{hp\pi}{m}, \quad h=0,1,\ldots,m$$

where

$$\varepsilon_p = \begin{cases} 1, & 0<p<m \\ \frac{1}{2}, & p=0,m \end{cases}.$$

Note: $P_x^{(h)} = P_x(w_h) = P_x\left(\frac{h\pi}{m\Delta t}\right)$.

Step 6. The raw estimates of the power spectrum are then smoothed by "hamming".

$$SP_x^{(0)} = 0.54P_x^{(0)} + 0.46P_x^{(1)} .$$

$$SP_x^{(h)} = 0.23P_x^{(h-1)} + 0.54P_x^{(h)} + 0.23P_x^{(h+1)}, \quad 0<h<m.$$

$$SP_x^{(m)} = 0.54P_x^{(m)} + 0.46P_x^{(m-1)} .$$

Step 7. A check sum is computed to check the computations of the estimates.

$$CHKSUM = \frac{\pi}{m\Delta t}\left[\frac{1}{2}(SP_x^{(0)} + SP_x^{(m)}) + \sum_{h=1}^{m-1} SP_x^{(h)}\right].$$

This should equal $R_x^{(0)}$, the autocovariance at zero lag.

Step 8. To compensate for the prewhitening in Step 2, the smoothed spectrum is recoloured by

$$RSP_x^{(h)} = SP_x^{(h)} /(1 + C^2 - 2C\cos w_h\Delta t), \quad h=0,1,\ldots,m.$$

Similarly, Steps 1 to 8 can be applied to series Y.

Step 9. The cross-covariance is computed by the formula

$$R_{xy}^{(p)} = \frac{1}{n-p}\sum_{q=1}^{n-p} X_q Y_{q+p}, \quad p=0,1,2,\ldots,m.$$

$$R_{xy}^{(-p)} = \frac{1}{n-p}\sum_{q=1}^{n-p} X_{q+p} Y_q, \quad p=0,1,2,\ldots,m.$$

Step 10. (optional). In detrending the series

$$A_{xy}^{(p)} = R_{xy}^{(p)} - \beta - \alpha i, \quad i=0,1,\ldots,n-1,$$

where α and β are defined in Step 4.

Step 11. The cross spectrum, $P_{xy}^{(h)}$, is given by

$$P_{xy}^{(h)} = C_{xy}^{(h)} + iQ_{xy}^{(h)} .$$

The cospectrum is obtained from

$$C_{xy}^{(h)} = \frac{\Delta t}{\pi} \sum_{p=0}^{m} \varepsilon_p \left(R_{xy}^{(p)} + R_{xy}^{(-p)}\right) \cos\frac{hp\pi}{m} .$$

The quadrature spectrum is obtained from

$$Q_{xy}^{(h)} = \frac{\Delta t}{\pi} \sum_{p=0}^{m} \varepsilon_p \left(R_{xy}^{(p)} - R_{xy}^{(-p)}\right) \sin\frac{hp\pi}{m} .$$

$h=0,1,2,\ldots,m.$

$$\varepsilon_p = \begin{cases} 1 & , \quad 0<p<m \\ \frac{1}{2} & , \quad p=0,m \end{cases} .$$

Step 12. Both the cospectrum and quadrature spectrum are smoothed by "hamming" as shown in Step 6.

Step 13. The amplitude and phase of the cross-spectrum are computed.

$$AM_{xy}^{(h)} = \sqrt{\left(SC_{xy}^{(h)}\right)^2 + \left(SQ_{xy}^{(h)}\right)^2} .$$

$$PHAS_{xy}^{(h)} = \operatorname{Arg}\left(SC_{xy}^{(h)} + iSQ_{xy}^{(h)}\right) .$$

The phase angle computed is the phase shift of series Y with respect to series X.

Step 14. The transfer function from series X to Y is given by

$$T_{xy}^{(h)} = \frac{P_{xy}^{(h)}}{P_x^{(h)}} = TAM_{xy}^{(h)} \, e^{iPHAS_{xy}^{(h)}}$$

The amplitude is given by

$$TAM_{xy}^{(h)} = AM_{xy}^{(h)} / SP_x^{(h)} .$$

The phase shift from X to Y is the same as that of the cross-spectrum. Both the transfer function amplitudes from X to Y and Y to X are printed.

Step 15. Finally the coherence squared between X and Y is given as

$$COSQ_{XY}^{(h)} = (AM_{XY}^{(h)})^2 / SP_X^{(h)} . SP_Y^{(h)} .$$